Remarks

Claims 1-16, 18, and 20-34 are pending in this application. Claims 1-16, 18, 20, and 30-33 are subject to active examination; claims 21-29 and 34 were previously withdrawn. With this response, Applicants cancel claims 18, 20-29, and 34 and amend claims 1 and 30-32 to more clearly define the claimed subject matter. Support for these amendments may be found, e.g., in the original claims.

The specification and sequence listing have been amended to provide the sequences of BCMA and TACI. Support for these amendments can be found at paragraph [0006].

Objection to the Title

The Examiner states that the title, "Therapeutic Regimens for BAFF Antagonists," is not descriptive. The Examiner suggests amending the title to "A Method for Treating an Autoimmune Disease Comprising Administering a BAFF Antagonist."

Applicants respectfully submit that the current title is descriptive. Indeed, it is more descriptive of the claimed subject matter than the new title proposed by the Examiner. The claims are not limited to treating autoimmune disease; they also recite, e.g., treating a patient having an immunologic disorder (claim 1) and inhibiting generation of pathogenic B cells (claim 32). On the other hand, all of the claimed methods relate to a common treatment regimen: administering a BAFF antagonist, temporarily discontinuing the administration, and repeating these steps at least once. Thus, "Therapeutic Regimens for BAFF Antagonists" describes the claimed subject matter.

Claim Objections

Amended claims 1 and 30-32 do not recite a soluble BAFF receptor, rendering moot the Examiner's objection that these claims recite a non-elected invention.

The amended claims do not recite any abbreviations. Thus, the Examiner's suggestion that the "syntax of claim 1 can be improved by describing a term first followed by an abbreviated form of the description in a parenthesis (e.g., B cell activating factor (BAFF))" is moot.

Written Description

The Examiner has rejected claims 1-6, 8, 15-16, 18, and 30-33 for allegedly failing to comply with the written description requirement of 35 U.S.C. § 112, first paragraph. The Examiner states that the claims contain subject matter which was not described in the specification in such a way as to reasonably convey to one skilled in the relevant art that Applicants had possession of the claimed invention when the application was filed.

Applicants maintain that the previously pending claims were adequately described. The Examiner's argument for lack of written description of the term "anti-BAFF receptor antibody" recited in the previously pending claims is based on a misunderstanding of the term "BAFF." The Examiner seems to believe that "B cell activating factor" is a functional description of a genus of molecules and that the term "BAFF" is merely an abbreviation of that purely functional language. Thus, the Examiner states that "BAFF as broadly interpreted includes all functional equivalents regardless of structure . . . [m]ere function (B cell activating factor receptor) does not describe the structure of a receptor . . . the term 'B cell activating' as being used instantly does not distinguish one activating factor from another." Following this faulty

premise, the Examiner concludes that the recited "BAFF receptor" is "claimed by function alone."

In the art, however, "BAFF" refers to a specific protein, and "B cell activating factor belonging to the TNF family" merely describes the origin of the term. See, e.g., Schneider et al., *J. Exp. Med.* 189:1747-1756 (1999). Three proteins have been identified to date as BAFF receptors: TACI, BCMA, and BAFFR (also known as BR3) (see paragraph [0006] of the instant specification). Thus, the recited antibodies are described by binding to fully-characterized antigens. As recognized by the Federal Circuit and the PTO's own guidelines, the written description requirement requires nothing more. In particular, the specification need not describe an actual reduction to practice of an antibody that binds to the recited antigen, where the antigen is fully-characterized. See *Noelle v. Lederman*, 355 F.3d 1343, 1349, 69 USPQ2d 1508, 1514 (Fed. Cir. 2004); see also Example 13 of the PTO's Written Description Training Materials.

Applicants also note that although there is no such requirement, antibodies against BAFF receptors are disclosed in the specification; others were known in the art. See paragraphs [0050] and [0051]; see also US 2003/012783.

In the interests of advancing prosecution, however, Applicants have amended the claims to recite an antibody that binds to SEQ ID NO:1 (BAFF-R), SEQ ID NO:7 (BCMA), or SEQ ID NO:8 (TACI). Applicants submit that the written description rejection is moot and request that it be withdrawn.

Enablement

The Examiner has rejected claims 1-6, 8, 15-16, 18, and 30-33 for allegedly failing to comply with the enablement requirement of 35 U.S.C. § 112, first paragraph.

The Examiner states that the claims contain subject matter which was not described in the specification in such a way as to enable one skilled in the art to make and/or use the invention.

Applicants respectfully submit that the specification fully enables the skilled artisan to practice the claimed methods. As noted by the Examiner, In re Wands sets forth 8 factors to be considered in determining whether undue experimentation would be required. The Examiner bears the burden to provide reasons why the specification is not enabling. M.P.E.P. § 3404.04. Proper analysis of the Wands factors reveals that the Examiner has not met that burden.

The nature of the invention and the breadth of the claims

The invention relates to specific regimens for timing the administration of antibodies against BAFF-R, BCMA, or TACI to a patient having an immunological disorder. The Examiner has ignored this aspect of the claims throughout the Office Action and especially in the context of the enablement rejection. Indeed, the Examiner states that the claims "are broadly drawn to a method of treating a patient having any immunological disorder comprising administering a therapeutically effective amount of any anti-BAFF receptor antibody." Applicants do not purport to have invented all methods of treating an immunological disorder comprising administering an antibody against a BAFF receptor. It was already well-established in the art that BAFF antagonists could be used to treat immunological disorders. The nature of the invention is in the timing of administration of the BAFF antagonist.

The state of the prior art and the predictability or lack thereof in the art

The art teaches that the SNF1 mouse is a well-established model of systemic lupus erythematosus (SLE) and closely mimics many important features of human SLE. Like human SLE patients, these mice exhibit high titers of IgG anti-dsDNA and anti-glomerular antibodies, accompanied by severe glomerulonephritis. SNF1 mice also share the female bias in disease prevalence observed in humans. Many peer-reviewed journal articles are based on experimental studies using these mice. See, e.g., Kang et al., J. Immunol. 174:3247-55 (2005); Kalled et al., J. Immunol. 160:2158-65 (1998).

The amount of guidance present and the presence or absence of working examples

The specification includes a wealth of in vivo data supporting the claimed methods. As noted above, the SNF1 mouse is a well-established animal model that exhibits many of the hallmarks of human SLE. Applicants have shown that short-term administration of a BAFF antagonist to nephritic SNF1 mice with mild-to-moderate SLE results in a long-term clinical benefit. Perhaps most importantly, 100% of treated mice survived to 49 weeks, whereas only 30% of control mice remained alive (Example 1). Treatment also significantly reduced progression of disease to severe nephritis, whether assessed by proteinuria levels or by histology (Example 2). Short-term administration of a BAFF antagonist also inhibited cardiac inflammation (Example 3), B cell hyperplasia (Example 4), and production of autoantibody (Example 5). Finally, the treatment reduced the percentage of $IgM^{-}IgD^{+}$ B cells, which are presumed to be pathogenic (Example 6).

These data show that short-term administration of a BAFF antagonist not only reduces the severity of various markers of disease progression, it dramatically

increases survival. The benefits of the treatment appear to persist well after its administration in the first 4 weeks of the study. Thus, the Examples provide powerful evidence that an immunological disease can be treated using a regimen in which a BAFF antagonist is administered for a relatively short period, followed by a longer period in which the administration is discontinued.

The quantity of experimentation needed

Relatively little experimentation would be needed to determine whether the claimed treatment regimen is effective as applied to any particular antibody. The skilled artisan, already familiar with the SNF1 model system, could follow Applicants' teachings to determine whether the therapeutic benefits shown in the Examples are also obtained with the antibody of interest.

Relative skill of those in the art

The level of skill in the art is high: one of ordinary skill presumably has an M.D. or Ph.D. and years of experience developing treatments for immunological disorders. Applicants respectfully note that the Examiner has ignored this factor, in contravention of M.P.E.P. § 2164.01(a).

In conclusion, Applicants submit that proper consideration of all of the Wands factors strongly supports the conclusion that the specification enables the claimed methods. Accordingly, Applicants request reconsideration and withdrawal of the enablement rejection.

Obviousness-type Double Patenting

The Examiner has provisionally rejected claims 1, 5-6, 15, and 30-32 under the doctrine of obviousness-type double patenting as allegedly unpatentable over claims

60, 61, and 75-80 of U.S.S.N. 11/065,669. Despite acknowledging that the allegedly conflicting claims are not identical, the Examiner states that they are not patentably distinct from each other.

As an initial matter, Applicants note that the cited application is no longer co-pending. It is abandoned, rendering the rejection moot.

Even if U.S.S.N. 11/065,669 were co-pending, however, the rejection would still be improper, as applied to both the previously pending claims and the currently amended claims. The instant application should be treated as the later-filed application: its earliest priority claim is to U.S.S.N. 60/512,880 (filed October 20, 2003); whereas U.S.S.N. 11/065,669 is a continuation of U.S.S.N. 10/045,574 (filed November 7, 2001). Since the application at issue was filed later than the application cited under the doctrine of obviousness-type double patenting, the test is "whether the invention defined in a claim in the application would have been anticipated by, or an obvious variation of, the invention defined in a claim" of the cited co-pending application. See M.P.E.P. § 804. The analysis mirrors that of 35 U.S.C. § 103; the Examiner must show that the co-pending application renders obvious each element of the claim rejected in the application at issue. Id. The claims of the instant application (both as previously pending and as currently amended) relate to a method of treatment comprising (a) administering an agent; (b) discontinuing the administration for 8, 9, 10, 11, or 12 weeks or longer; and (c) repeating steps (a) and (b) at least once. The Examiner does not argue that the cited application renders these steps of the claimed methods obvious. Indeed, the Office Action does not even mention this series of steps. Thus, the rejection is improper and should be withdrawn.

Conclusion

In view of the foregoing amendments and remarks, Applicants respectfully request the reconsideration and withdrawal of the pending rejections and objections.

Please grant any additional extensions of time required to enter this response and charge any additional fees to deposit account 06-0916.

Respectfully submitted,

FINNEGAN, HENDERSON, FARABOW,
GARRETT & DUNNER, L.L.P.

Dated: March 12, 2009

By: 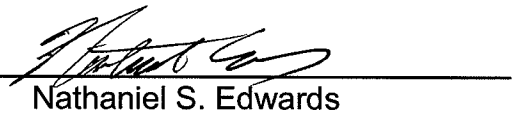

Nathaniel S. Edwards
Reg. No. 57,745
Tel.: 617.452.1669

Attachment 3

Anti-CD40 Ligand Antibody Treatment of SNF_1 Mice with Established Nephritis: Preservation of Kidney Function[1]

Susan L. Kalled,[2]* Anne H. Cutler,* Syamal K. Datta,† and David W. Thomas*

Prior studies have demonstrated that treatment of young, prenephritic lupus-prone mice with Ab directed against CD40 ligand (CD40L) prolongs survival and decreases the incidence of severe nephritis. In this report, we show that for (SWR × NZB)F_1 (SNF_1) animals with established lupus nephritis, long-term treatment with anti-CD40L beginning at either 5.5 or 7 mo of age prolonged survival and decreased the incidence of severe nephritis. "Older" mice were chosen for these studies to more closely resemble the clinical presentation of patients with established renal disease. We show that age at the start of treatment, which typically correlates with severity of disease, is an important factor when determining an efficacious therapeutic protocol since animals that began treatment at 7 mo of age required a more aggressive treatment protocol than animals at 5.5 mo of age. Remarkably, several anti-CD40L-treated animals beginning treatment at age 5.5 mo demonstrated a decline in proteinuria, as opposed to increasing proteinuria levels seen in hamster IgG (HIg)-treated controls, and histologic examination of kidneys from anti-CD40L-treated mice revealed dramatically diminished inflammation, sclerosis/fibrosis, and vasculitis, in marked contrast to the massive inflammation and kidney destruction observed in control animals that received hamster IgG. Spleens from anti-CD40L-treated mice also exhibited markedly reduced inflammation and fibrosis compared with controls. Together, these results show that treatment of older, nephritic SNF_1 animals with long-term anti-CD40L immunotherapy significantly prolongs survival, reduces the severity of nephritis, and diminishes associated inflammation, vasculitis, and fibrosis. *The Journal of Immunology,* **1998, 160: 2158–2165.**

Systemic lupus erythematosus (SLE)[3] is a spontaneously arising autoimmune disease with a female predominance and is characterized by the production of a variety of pathogenic anti-nuclear autoantibodies (1). In lupus nephritis, kidney damage is mediated by both cellular and humoral immune mechanisms, including the formation of immune complexes that deposit in kidney glomeruli and activate the complement cascade resulting in glomerulonephritis. It has previously been established that the production of anti-nuclear autoantibodies in both human and mouse SLE is driven by cognate interactions between select populations of autoimmune Th cells and B cells (2–4). Autoantibody-inducing Th cells have been cloned from (SWR × NZB)F_1 (SNF_1) mice with lupus nephritis as well as from nephritic patients with SLE (5–9), and such clones from the SNF_1 model rapidly induce immune-deposit glomerulonephritis when transferred into young preautoimmune mice. In the absence of these Th cells, the autoantibody-producing B cells are not sustained and presumably undergo apoptosis.

Critical to the production of Ab against T-dependent Ags is the interaction between CD40L on Th cells and its receptor, CD40, on the cognate B cell. This interaction is essential for germinal center formation, B cell proliferation and differentiation, isotype switching, and generation of B cell memory (reviewed in 10). CD40-CD40L interaction is also important for T cell activation since T cells require costimulatory signals through molecules that are upregulated upon CD40-CD40L engagement. CD40-CD40L interaction has been shown to be important for several experimentally induced autoimmune diseases, such as collagen-induced arthritis (11), experimental allergic encephalomyelitis (EAE) (12), oophoritis (13), as well as graft-vs-host disease (14, 15), since induction of all of these diseases can be blocked with anti-CD40L treatment at the time of Ag administration. In addition, CD40-CD40L interaction appears to be critical for the production of pathogenic autoantibodies in spontaneous murine lupus. Blocking this interaction, even briefly (for 1 wk) in young, prenephritic SNF_1 lupus animals with anti-CD40L therapy produced unexpected long-term benefit, such as increased survival and diminished incidence of severe nephritis at 12 mo of age (16). Similar results were seen in the NZB/NZW lupus model with long-term anti-CD40L therapy (6 mo) (17).

Given the results from these numerous studies, there has been much speculation as to the potential usefulness of a mAb directed against the human CD40L molecule in treatment of autoimmune disease. What is lacking is data that show efficacy of anti-CD40L Ab in established renal disease, both moderate and severe. With this in mind, we designed studies using SNF_1 mice that would resemble the stage of disease with which patients with established lupus nephritis could present for initial diagnosis and treatment. In this study, we report the effects of anti-CD40L therapy on animals that began treatment at 5.5 or 7 mo of age, receiving an initial regimen of anti-CD40L Ab for several weeks, followed by monthly dosing for the duration of the study. Anti-CD40L immunotherapy resulted in prolonged survival, decreased autoantibody levels, and diminished proteinuria, indicating an arrest of established disease. Anti-CD40L-treated mice also exhibited reduced renal inflammation, cellular proliferation, vasculitis, and sclerosis/fibrosis, as well as diminished inflammation and fibrosis in the

*Department of Immunology, Biogen Inc., Cambridge, MA 02142; †Departments of Medicine, Microbiology-Immunology, and Multipurpose Arthritis Center, Northwestern University Medical School, Chicago, IL 60611

Received for publication July 29, 1997. Accepted for publication November 7, 1997.

The costs of publication of this article were defrayed in part by the payment of page charges. This article must therefore be hereby marked *advertisement* in accordance with 18 U.S.C. Section 1734 solely to indicate this fact.

[1] S.K.D. is supported by grants from the National Institutes of Health (RO1-AI41985 and AR39157) and The Arthritis Foundation.

[2] Address correspondence and reprint requests to Dr. Susan L. Kalled, Department of Immunology, Biogen Inc., 14 Cambridge Center, Cambridge, MA 02142.

[3] Abbreviations used in this paper: SLE, systemic lupus erythematosus; CD40L, CD40 ligand; SNF_1, (SWR × NZB)F_1; HIg, hamster IgG; H&E, hematoxylin-eosin.

0022-1767/98/$02.00

spleen. Lastly, in contrast to 5.5 month-old mice, 7 month-old animals beginning treatment for the first time required more frequent dosing of anti-CD40L in the first 12 wk to establish efficacy, most likely because of components of advanced disease that are not currently understood.

Materials and Methods

Mice

SWR and NZB mice were purchased from The Jackson Laboratory (Bar Harbor, ME). (SWR × NZB)F_1 (SNF_1) hybrids were bred in the animal facility at Biogen under conventional barrier conditions. Female SNF_1 mice were used for all studies.

Antibodies

The MR1 hybridoma (18), which produces Armenian hamster anti-mouse CD40L Ab, was purchased from the American Type Culture Collection (Rockville, MD). The hybridoma Ha4/8-3.1, an Armenian hamster IgG mAb specific for keyhole limpet hemocyanin, was kindly provided by Dr. Donna Mendrick (Human Genome Sciences Inc., Rockville, MD). Both mAbs were purified from culture supernatant on a protein A Fast Flow column (Pharmacia Biotech, Piscataway, NJ).

Treatment protocols

All injections were given i.p. Each study consisted of a control group that received Ha4/8-3.1 and a treated group that received anti-CD40L mAb. Animals received in the first week 250 μg of Ab on days 1, 3, and 5, then a single dose of 500 μg of mAb once per wk for either 6 or 12 wk as indicated in the text, followed by a single injection of 500 μg monthly until death of the animal or termination of the study. Studies began when animals were either 5.5 mo or 7 mo of age.

ELISA assays

For total Ig and anti-anti-CD40L ELISAs, ELISA plates (Corning Glass Works, Corning, NY) were coated overnight at 4°C with 5 μg/ml of goat anti-mouse IgG+IgM (Jackson ImmunoResearch, West Grove, PA) and anti-CD40L, respectively. After blocking, serial serum dilutions were added, followed by the detection Ab, biotin-conjugated donkey anti-mouse IgG (H+L) (Jackson ImmunoResearch), and streptavidin-horseradish peroxidase (SA-HRP) reagent (Southern Biotech, Birmingham, AL). The developing reaction was stopped by adding 2N sulfuric acid. Plates were read at an OD of 450 nm, and a standard curve was generated using known quantities of purified whole mouse Ig (Jackson ImmunoResearch). Anti-ssDNA and anti-dsDNA ELISAs were performed using NUNC-Immuno Plate MaxiSorp plates (NUNC A/S, Denmark). Plates were coated overnight at 4°C first with 100 μg/ml methylated BSA (Calbiochem Corp, La Jolla, CA), then with 50 μg/ml grade I calf thymus DNA (Sigma, St. Louis, MO). The calf thymus DNA was sheared by sonication and then digested with S1 nuclease before use. For the anti-ssDNA assay, the DNA was boiled for 10 min and chilled on ice before use. After blocking, serial dilutions of serum samples were added and incubated at room temperature for 2 h. Autoantibodies were detected with goat anti-mouse IgG-AP (Sigma) and developed with *p*-nitrophenyl phosphate (Sigma) in 1 M diethanolamine buffer. Plates were read at an OD of 405 nm, and standard curves were obtained by using known quantities of anti-DNA mAb 205, which is specific for both ss- and dsDNA (2).

Assessment of renal disease

The urine of each mouse was monitored weekly with Albustix (Bayer Corp., Terrytown, NY) to measure proteinuria. Proteinuria level is scored as follows: 0.5^+, 15 to 30 mg/dl ; 1^+, 30 mg/dl; 2^+, 100 mg/dl; 3^+, 300 mg/dl; 4^+, >2000 mg/dl.

The overall score for histopathologic grading of lupus nephritis is described elsewhere (19, 20) and was based on glomerular, interstitial, and tubular changes. The grades 0 to 4^+ are based on percent involvement of the structure being examined (i.e., glomeruli, vessels, etc.). Kidneys without lesions were graded as "0," and all tissue samples were coded and read blind.

Immunohistochemistry

Kidneys and spleens were fixed in 10% buffered formalin and embedded in paraffin. Five-millimeter cryostat sections were baked at 55°C, deparaffined, hydrated in ethanol, and stained with hematoxylin-eosin (H&E) for histologic examination or used for immunohistochemical staining. Briefly, sections were incubated first with a mAb that detects a cytoplasmic protein specific to reticular fibroblasts, ER-TR7 (Serotec, Oxford, UK) for 30 min at room temperature, washed with PBS, incubated with mouse anti-rat IgG (H&L) $F(ab)_2$ for 30 min at room temperature (Jackson ImmunoResearch, West Grove, PA), and visualized using the substrate 3,3′ diaminobenzidine (DAB) (Vector Laboratories, Inc., Burlingame, CA). Sections were counterstained with a 25% Wright-Giemsa (Fisher Diagnostics, Pittsburgh, PA) solution. Endogenous peroxidase activity was blocked using 2% hydrogen peroxide in methanol for 20 min before staining with the primary Ab. Photographs were taken on a Zeiss Axioplan photomicroscope at magnifications of ×100 and ×400.

Statistical analysis

Survival curves were estimated by life-table methodology, and groups were compared by the Wilcoxon test (21). The proportion of mice with $\geq 3^+$ (≥300 mg/dl) proteinuria was analyzed by a χ^2 test. Histopathologic renal scores were analyzed by a Wilcoxon two-sample test. Comparison of autoantibody levels was analyzed by Student's *t* test.

Results

Long-term anti-CD40L therapy beginning at 5.5 mo of age significantly prolongs survival of SNF_1 mice

Seven SNF_1 mice, beginning at 5.5 mo of age, were treated in the first week with 250 μg of either anti-CD40L mAb or control hamster IgG on days 1, 3, and 5 followed by a weekly injection of 500 μg for 5 consecutive wk, then monthly injections of 500 μg until death of the animal or termination of the study. By ~10 mo of age (4.5 mo after the start of treatment), 6 of 7 (85.7%) control animals had died, whereas no anti-CD40L-treated animals had died (Fig. 1*A*). By 13 mo of age (7.5 mo after start of treatment) no control animals remained alive, yet all anti-CD40L-treated animals were alive. In fact, these animals appeared healthy up to 15.5 mo of age when the study was terminated and all animals, except one, were euthanized for histopathology (one mouse died during a kidney biopsy at ~13 mo of age and was not included in the survival timepoints of Figure 1*A* or statistics beyond 13 mo). As HIg-treated controls became moribund, the animals were euthanized and their organs removed for histology. Overall, anti-CD40L-treated mice demonstrated a survival rate significantly different ($p < 0.001$) from HIg-treated controls.

Long-term anti-CD40L therapy beginning at age 5.5 mo significantly inhibits development of severe nephritis, renal vasculitis, and fibrosis

Consistent with the prolonged survival effect of anti-CD40L therapy described above, this treatment also significantly inhibited the development of severe nephritis, defined as a proteinuria level of $\geq 3^+$ ($p < 0.001$ at all timepoints). As seen in Figure 1*B*, only 1 of 7 anti-CD40L-treated animals developed $\geq 3^+$ proteinuria by 13 mo of age whereas controls rapidly developed 4^+ proteinuria within 1 mo after treatment began (although 2 animals had 4^+ proteinuria when the study began due to a random assignment of groups). Remarkably, the proteinuria levels of 6 of 7 (85.7%) anti-CD40L-treated mice declined. This decline began as early as 3 mo after the start of treatment in some cases and as late as 6 mo in others.

Since anti-CD40L immunotherapy resulted in a decline in proteinuria, we asked if the severity of glomerulonephritis was also reduced as compared with controls. For this purpose, H&E-stained kidney tissue sections were read and scored blind to assess renal morphology and pathology. An example of normal kidney structure is seen in Figure 2*a*, a kidney section from an SWR female mouse, the normal parent of the (SWR × NZB) cross. Glomeruli are numerous, distinct with patent capillaries, normal cellularity, and architecture, and tubules are compact and of normal shape. In comparison, kidney sections from HIg-treated SNF_1 mice (Fig. 2*b*)

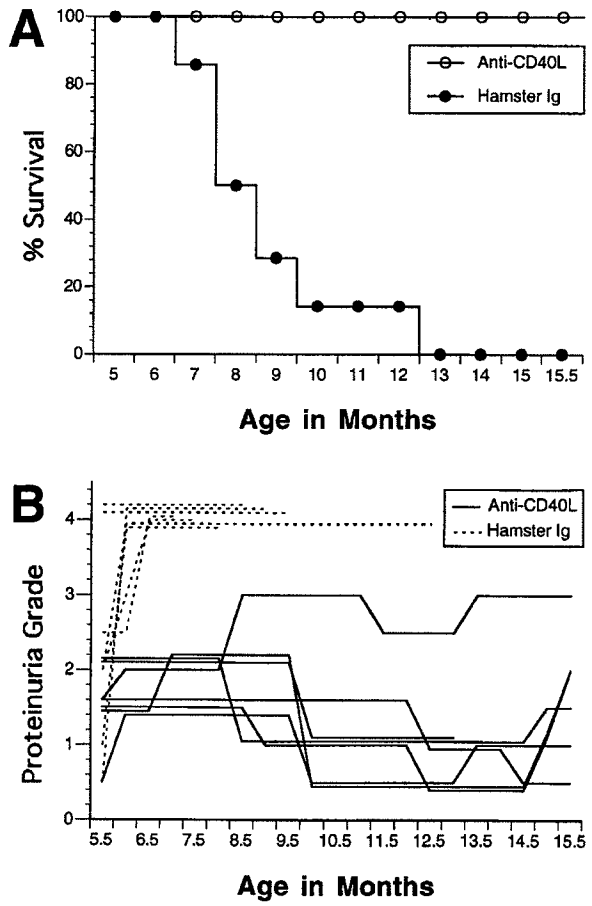

FIGURE 1. Effect of anti-CD40L immunotherapy beginning at 5.5 mo of age on survival and proteinuria in SNF_1 mice. *A*, The survival curves of anti-CD40L-treated and HIg controls differ significantly ($p < 0.001$ by Wilcoxon test). Control mice receiving HIg die rapidly with the onset of severe nephritis, and all but one are dead by age 12 mo while all anti-CD40L-treated mice are alive when the study is terminated at age 15.5 mo (except one mouse that died during a biopsy procedure at ~13 mo of age). *B*, Urine was monitored weekly for proteinuria as described in *Materials and Methods*. The proportion of mice with $\geq 3^+$ proteinuria differed significantly between anti-CD40L-treated and HIg controls at all timepoints ($p < 0.001$ by χ^2 test). Controls that did not have $\geq 3^+$ proteinuria at the start of treatment became 4^+ soon after, as opposed to anti-CD40L-treated mice where the proteinuria levels of six of seven mice declined and only one mouse developed 3^+ proteinuria.

exhibited severe disruption of kidney architecture, lesions involving all glomeruli, massive perivascular lymphoid accumulations, and tubular atrophy or dilation with proteinaceous casts. The glomeruli in these animals were enlarged and exhibited hypercellularity with crescents, hyaline deposits effacing capillary loops, thickening of capillary loops, basement membrane as well as mesangial thickening, and significant glomerular sclerosis. In stark contrast to the HIg-treated animals, tissue sections of kidneys from anti-CD40L-treated animals (Fig. 2*c*) revealed that, in general, the overall structural integrity of the kidneys was intact. Anti-CD40L-treated animals at age 15.5 mo had no to moderate (0 to 2^+) glomerulonephritis, except one mouse that developed 2 to 3^+ disease, and only 3 animals exhibited rare sclerotic glomeruli. Mouse CLR, which died at ~13 mo of age due to complications from a kidney biopsy procedure, had no obvious sign of glomerulonephritis in the biopsied tissue (Table I). Furthermore, most animals had no or

Table I. *Anti-CD40L therapy inhibits lupus-associated renal disease*

	Histopathologic Grading of Lupus Nephritis[a]		
Mouse[b]	Overall Score	Sclerosis/Fibrosis	Vasculitis
CR	1^+–2^+	0–1^+	1^+
CL	2^+	0–1^+	ND[c]
CN	2^+–3^+	0–1^+	2^+
CLR	0	0	ND
DR	2^+	0	0–1^+
DL	2^+	0–1^+	1^+–2^+
DN	0	0	0
HIg-control[d]	4^+	4^+	4^+

[a] 0 to 4^+ scoring was based on assessment described elsewhere (19, 20). The differences between anti-CD40L-treated and control mice were significant for overall, sclerosis-fibrosis, and vasculitis scores ($p < 0.01$ for all by Wilcoxon two-sample test).

[b] CR, CL, CN, CLR, DR, DL, DN all received anti-CD40L therapy beginning at age 5.5 mo. Kidney sections were prepared at age 15.5 mo except CLR, which is a biopsy sample at age 13 mo.

[c] ND, vasculitis could not be assessed because of a lack of arterioles in histologic sections.

[d] Five out of seven mice that received control HIg beginning at age 5.5 mo had identical histopathologic scores; therefore, one set of scores is given to represent all five. The two remaining mice died before tissues could be obtained.

only mild interstitial infiltration of mononuclear cells, although 2 of 7 animals had moderate infiltration. A comparison of the overall renal histopathologic scores for anti-CD40L-treated mice and the controls shows a significant difference in severity of glomerulonephritis by the Wilcoxon two-sample test ($p < 0.01$).

Consequences of interstitial infiltration include the activation of a variety of cell types and release of cytokines/growth factors resulting in fibrosis (22, 23), an overproduction of extracellular matrix components, and proliferation of normally quiescent cells, such as fibroblasts, which can lead to irreversible tissue damage. The presence of sclerosis/fibrosis was assessed by histologic examination of H&E-stained kidney sections (Table I), and comparison of the difference in incidence and severity of sclerosis/fibrosis between anti-CD40L-treated and control mice was found to be significant ($p < 0.01$) To further examine the effect of anti-CD40L therapy on the development of fibrosis, kidney tissue sections were analyzed with the mAb ER-TR7. This mAb recognizes reticular fibroblasts and stains the connective tissue of many organs. (Note: this Ab stains normal connective tissue strongly on frozen tissue sections. The tissue sections used in this report have been embedded in paraffin, resulting in a barely detectable staining, except in instances of damaged and fibrotic tissue.) In a kidney tissue section of the normal parent, SWR, no staining is detected in the kidney cortex (Fig. 2*d*). In HIg-treated animals, however, this Ab stained intensely the areas surrounding dilated tubules, interstitial infiltrate, and sclerotic glomeruli (Fig. 2*e*). Tissue sections of kidneys from anti-CD40L-treated animals exhibited no ER-TR7 staining above what was seen for controls (Fig. 2*f*). Additionally, examination of H&E-stained kidney sections revealed that, compared with HIg-treated mice that developed severe vasculitis, the severity of vasculitis in anti-CD40L-treated animals was significantly diminished ($p < 0.01$; Table I).

Long-term anti-CD40L therapy beginning at age 5.5 mo reduces splenic inflammation and inhibits development of fibrosis

Since animals in this lupus model develop splenomegaly, splenic tissue sections were examined to determine whether anti-CD40L therapy had any effect on inflammation/proliferation in the spleen, where hyperproliferation of autoantibody-producing B cells occurs. Normal splenic architecture can be seen in an H&E-stained

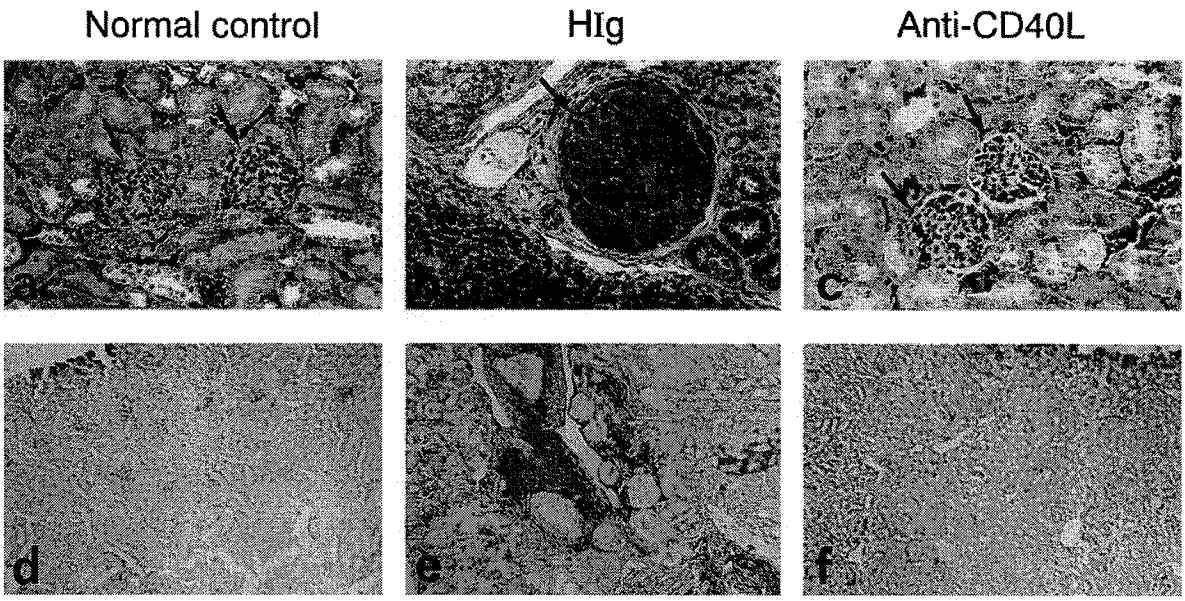

FIGURE 2. Renal histology from animals receiving long-term immunotherapy beginning at age 5.5 mo. Representative samples from the normal SWR parent (normal control), mice that received HIg (HIg) and anti-CD40L (anti-CD40L). Basic histology by H&E staining of kidney tissue sections (top row, ×400 magnification); arrows point to glomeruli. Examination of fibrosis by immunohistochemistry in kidney (bottom row, ×100 magnification). The brown staining represents detection of reticular fibroblasts. Sections were counterstained with Wright-Giemsa. The HIg sections are from the same animal that was 12.5 mo old at the time of death, and the anti-CD40L sections are from the same mouse at 15.5 mo of age.

tissue section of the normal parent, SWR, (Fig. 3*a*), where areas of red pulp and lymphocyte-containing white pulp are clearly discernible. The spleens of HIg-treated SNF_1 mice, however, often had such severe hyperplasia, accompanied by hyaline degeneration of the central follicular arterioles, that the typical H&E staining pattern distinguishing red and white pulp was completely disrupted and obscured, and there appeared to be a loss of white pulp altogether (Fig. 3*b*). There was also evidence of splenic necrosis in some animals. Splenic tissue sections from animals receiving anti-CD40L therapy revealed a marked expansion of the white pulp due to an increased number of follicles and expansion of what appeared to be dendritic-like cells. Nevertheless, no areas of necrosis were obvious, and inflammation and lymphoid proliferation were markedly reduced. In addition, anti-CD40L-treated mice exhibited

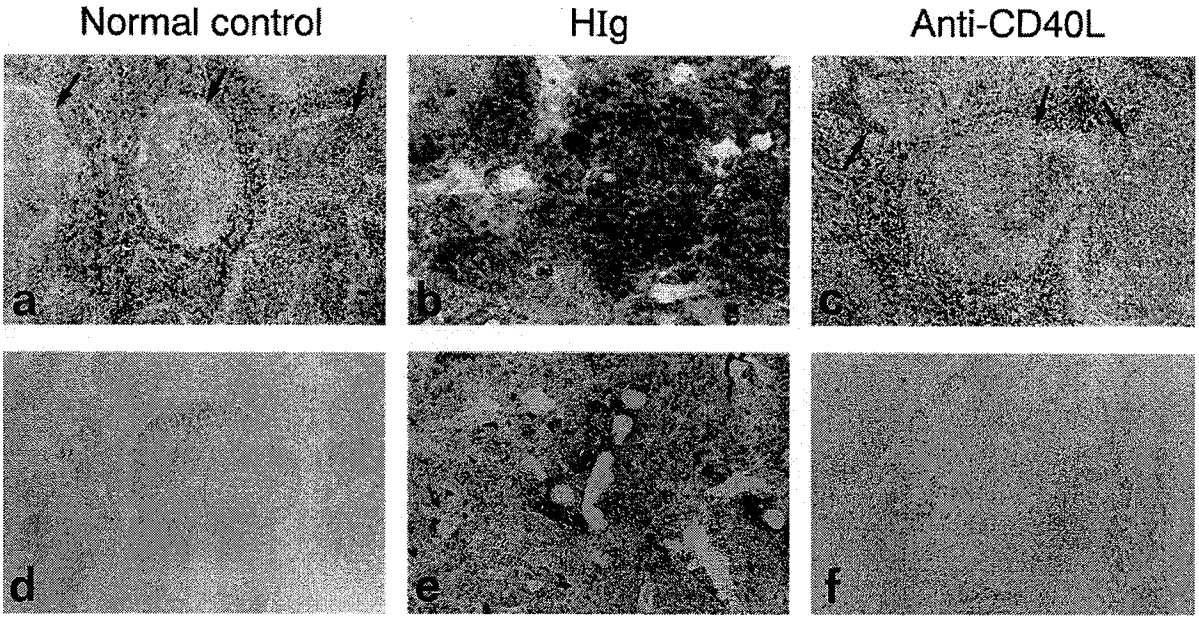

FIGURE 3. Splenic histology from animals receiving long-term immunotherapy beginning at age 5.5 mo. Representative samples from the normal SWR parent (normal control), mice that received HIg (HIg) and anti-CD40L (anti-CD40L). Basic histology by H&E staining of splenic tissue sections (top row, ×100 magnification); arrows point to areas of white pulp. Examination of fibrosis by immunohistochemistry in spleen (bottom row, ×100 magnification). The brown staining represents detection of reticular fibroblasts. Sections were counterstained with Wright-Giemsa. The HIg sections are from the same animal as in Figure 2, which was 12.5 mo old at the time of death. The anti-CD40L sections are from the same mouse as in Figure 2 and was 15.5 mo old when organs were taken for histology.

only rare, mild incidences of hyaline degeneration of central arterioles (Fig. 3*c*).

Splenomegaly is also characterized by fibrosis. To examine the extent of fibrosis in anti-CD40L-treated and control mice, splenic tissue sections were analyzed with the mAb, ER-TR7. In normal spleen this Ab stained very faintly within the red pulp only, the area containing splenic connective tissue (Fig. 3*d*). In the spleens of HIg-treated mice with active lupus, however, there was extensive staining with ER-TR7 not only in the red pulp, but extending into the white pulp as well, which appeared characteristic of periarterial fibrosis (Fig. 3*e*). In contrast, in sections from anti-CD40L-treated mice, there was typical faint staining in the red pulp, as seen in normal mice, and rare occasions of staining extending into the white pulp, thus indicating either no or only mild fibrosis in these animals (Fig. 3*f*).

SNF_1 lupus-prone mice beginning immunotherapy at 7 mo of age need a more aggressive anti-CD40L treatment protocol than 5.5 month-old animals

Since long-term immunotherapy with anti-CD40L proved so successful with animals that began treatment at 5.5 mo of age, this identical treatment regimen was repeated with older animals, 7 mo old, that typically have higher proteinuria levels as well as autoantibody titers. This treatment protocol, however, did not have any beneficial effect in older mice; anti-CD40L-treated animals developed severe nephritis and died at the same rate as controls (data not shown). We reasoned that more frequent anti-CD40L dosing early in therapy might be necessary given that the autoimmune response in these older animals is likely more robust than in younger mice. Therefore, 10 animals were given an extended weekly dosing regimen of 500 μg of either anti-CD40L or HIg for 12 consecutive wk followed by monthly injections of 500 μg/dose. This aggressive therapy significantly increased the survival rate of anti-CD40L-treated mice compared with controls ($p = 0.05$ by Wilcoxon test). At 10 mo of age (3 mo after start of therapy), only 20% of controls were alive compared with 80% of treated animals. At 13.5 mo of age the survival rate was 0% and 40% for control and anti-CD40L-treated animals, respectively, and at age 15.5 mo when the study was terminated two anti-CD40L-treated mice remained alive and appeared healthy (Fig. 4*A*).

The development/persistence of severe nephritis was assessed on a weekly basis by determining proteinuria levels; severe nephritis is defined as a proteinuria grade of $\geq 3^+$ ($\geq$300 mg/dl). The effect of anti-CD40L therapy on proteinuria levels in the 7 month-old mice was not as dramatic as that seen in animals that began treatment at age 5.5 mo, probably because 6 of 10 animals in the anti-CD40L-treated group had severe nephritis before the start of treatment. Regardless, when compared with HIg-treated animals (5 of 10 had severe nephritis before treatment), the proportion of anti-CD40L-treated mice with $\geq 3^+$ proteinuria differed significantly ($p < 0.001$) from controls at each timepoint analyzed except at 7.5, 8.5, and 10 mo (Fig. 4*B*). Furthermore, two anti-CD40L-treated animals exhibited a decline in proteinuria that remained at the diminished level for several mo (Fig. 4*B*).

Long-term anti-CD40L therapy reduces autoantibody production in SNF_1 mice

Autoantibodies, a hallmark of human SLE and the SNF_1 lupus model, are seen in increasing amounts as SNF_1 female mice age. After reaching a peak level, which in our colony is seen at approximately age 9.5 mo, detectable serum titers drop dramatically, probably due to immune complex deposition in the kidneys and other tissues. Serum levels of anti-ssDNA and anti-dsDNA autoantibodies were determined at regular intervals, and, regardless of

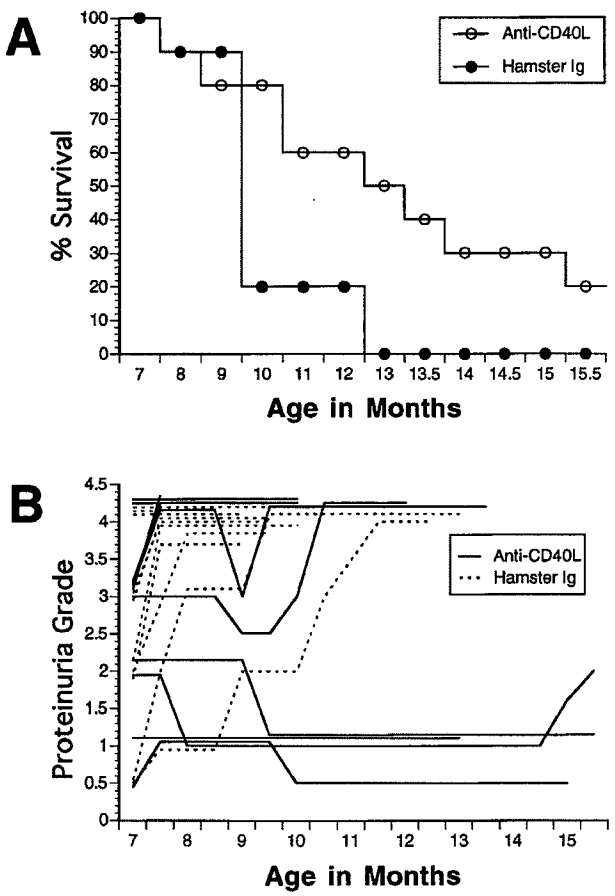

FIGURE 4. Effect of aggressive anti-CD40L immunotherapy beginning at age 7 mo on survival and proteinuria in SNF_1 mice. *A*, The survival curves of anti-CD40L-treated and HIg controls differed significantly ($p = 0.05$ by Wilcoxon test). HIg-treated mice exhibited a strong correlation between increasing age and rate of death, and all animals were dead by age 13 mo. Anti-CD40L-treated mice exhibited prolonged survival and at age 15.5 mo 2 of 10 mice remained alive. *B*, Urine was monitored weekly as described in *Materials and Methods*. The proportion of mice with $\geq 3^+$ proteinuria differed significantly ($p < 0.05$ by χ^2 test) between anti-CD40L-treated and HIg controls at all timepoints except 7.5 to 8.5 and 10 mo. Mice were assigned to receive either anti-CD40L or HIg according to their baseline proteinuria grade to create approximately equivalent treatment groups.

whether mice began anti-CD40L treatment at 5.5 or 7 mo of age, anti-CD40L therapy resulted in an overall reduction in the mean value of anti-ssDNA and anti-dsDNA autoantibody detected when compared with HIg-treated controls (Fig. 5). Most animals that began immunotherapy at age 5.5 mo had detectable autoantibody levels and, whereas the HIg-treated controls developed increased titers until age 9.5 mo, the mean values for anti-CD40L-treated mice remained low and in some cases declined. These differences were significant at the timepoints indicated in Figure 5 ($p < 0.05$ at 8.5 mo for both anti-ssDNA and anti-dsDNA). Mice that began treatment at age 7 mo also had detectable autoantibody titers at the start of therapy; however, the mean values of anti-ssDNA and anti-dsDNA autoantibodies for anti-CD40L-treated mice remained low or declined compared with controls, which continued to rise until approximately age 9.5 mo. These values differed significantly at certain timepoints (at 8.5 mo, $p = 0.06$ for anti-ssDNA and $p < 0.05$ for anti-dsDNA; at 9.5 mo, $p < 0.05$ for anti-dsDNA). Statistical analysis was not done for those timepoints where there were fewer than 2 control mice alive.

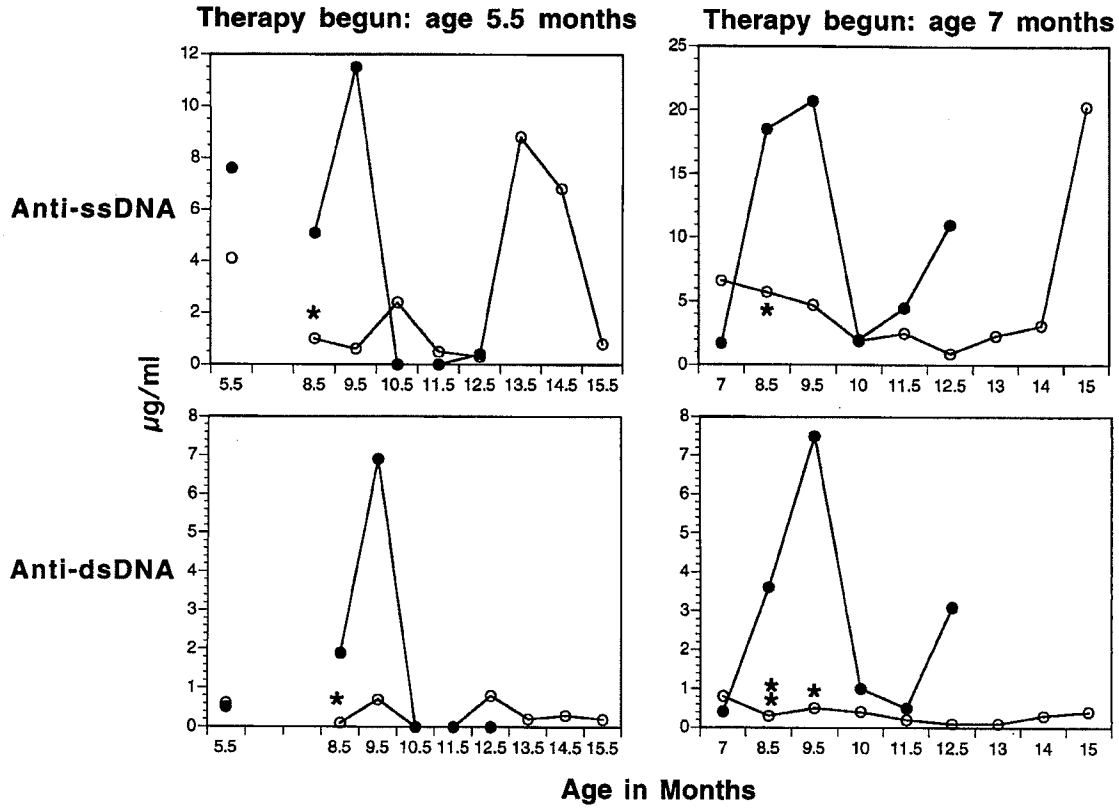

FIGURE 5. Effect of anti-CD40L immunotherapy on anti-ssDNA and anti-dsDNA autoantibody levels. Serum autoantibody levels were monitored monthly, except for mo 6 to 8 in animals beginning treatment at 5.5 mo of age. The geometric mean μg/ml of autoantibodies is shown for animals that received anti-CD40L (○) or HIg (●). An asterisk (*) denotes points at which the autoantibody levels differed significantly ($p < 0.05$ by Student's t test); a double asterisk denotes significance, $p = 0.06$. Statistical analysis was not performed at timepoints where the number of surviving control animals was less than 2.

Although it was expected that anti-CD40L treatment would serve to inhibit Ab responses in general, including anti-anti-CD40L Ab, animals in both studies did, in fact, develop such a response. For those mice that began anti-CD40L treatment at age 5.5 mo, three animals exhibited serum anti-anti-CD40L titers at 9.5 and 11.5 mo, and one animal exhibited titers at 11.5 and 14.5 mo (Table II). The response, however, was not persistent and the sporadic nature did not appear to adversely affect the animals since there was no parallel increase in proteinuria (Fig. 1*B*), and only 50% of mice had a correlative rise in autoantibody titers (Fig. 5). On the other hand, several animals that did not begin anti-CD40L treatment until age 7 mo developed an anti-anti-CD40L response within 2 mo of therapy, and it was persistent) in most cases (Table III). Two of eight surviving animals 1.5 mo after the start of therapy (age 8.5 mo) had developed an anti-anti-CD40L response, and this number increased to four of eight surviving mice at age 9.5 mo. For mice beginning immunotherapy at age 7 mo, there was a strong correlation between the animal having severe nephritis at the start of therapy, development of an anti-anti-CD40L response, and a lack of long-term survival.

Table II. *Anti-anti-CD40L response in mice that began treatment at age 5.5 months*

	Age in Months						
Mouse	8.5	9.5	10.5	11.5	12.5	13.5	14.5
CR	–[a]	–	–	–	–	–	–
CL	–	–	–	+	–	–	+
CN	–	+	–	+	–	–	–
CLR	–	+	–	+	–	ND[b]	ND
DR	–	+	–	+	–	–	–
DL	–	–	–	–	–	–	–
DN	–	–	–	–	–	–	–

[a] "–" indicates no detectable response; "+" indicates a detectable response.
[b] ND, not done since mouse died due to a biopsy complication at ≈13 mo of age.

Discussion

This work provides the first evidence that inhibiting the CD40-CD40L costimulatory pathway with an anti-CD40L mAb has a

Table III. *Anti-anti-CD40L response in mice that began treatment at age 7 months*

	Age in Months					
Mouse	8.5	9.5	11.5	12.5	14	15
XIDR	–[a]	–	–	–	+	+
XIDL	–	–	–	–	Ø[b]	
XIDN	Ø					
XIDLR	–	–	+	+	+	–
XIER	–	+	+	+	Ø	
XIEL	Ø					
XIEN	+	+	Ø			
XIELR	–	+	+	Ø		
XIFR	+	+	Ø			
XIFN	–	–	–	–	–	–

[a] "–" indicates no detectable response; "+" indicates a detectable response.
[b] "Ø" indicates the mouse died before this timepoint.

beneficial therapeutic effect in animals with established lupus nephritis. The impact of long-term anti-CD40L therapy on nephritic 5.5-month-old SNF_1 mice with proteinuria was a stabilization followed by a decline in proteinuria in six of seven animals, a significantly increased survival rate at age 15.5 mo, and decline in the incidence of severe glomerulonephritis, vasculitis, and fibrosis. These results show that anti-CD40L can function to arrest established renal disease and are striking, given that in this model SNF_1 females die of severe nephritis usually by age 12 mo (16, 24).

The hallmarks of interfering with the CD40-CD40L pathway, inhibiting Ig isotype switch and Ab production, have been demonstrated many times in various disease models, primarily, however, in a fashion that inhibited the onset of a humoral immune response. In general most SNF_1 animals, without therapeutic intervention, developed significant autoantibody titers as they aged, reaching a peak before disappearance from the periphery due to immune complex deposition in the kidneys and other tissues. Animals that received anti-CD40L immunotherapy, however, maintained consistently low autoantibody titers when compared with controls, often falling below baseline, which was determined just before the start of therapy. Nevertheless, an anti-anti-CD40L response in animals that began treatment at age 7 mo developed rather quickly and was persistent, unlike what was observed in mice that received treatment earlier, at age 5.5 mo, where such a response was sporadic among a few mice and apparently without consequence to disease progression. It is possible that with advanced disease select B cells no longer require a costimulatory signal through CD40, or they may function in a T-independent manner (25), making inhibition of the CD40-CD40L pathway inconsequential. Indeed, CD40L knockout/*lpr* mice can produce some autoantibodies and develop a markedly delayed and mild form of lupus (26).

Additionally, for mice not receiving anti-CD40L therapy until age 7 mo, increased dosing was necessary to establish efficacy. It was clear that animals with $\geq 3^+$ nephritis just before dosing did not benefit from treatment, most likely because of pre-existing kidney damage that was too severe and irreversible. Possible explanations for the need of a more aggressive anti-CD40L treatment regimen in 7-month-old animals are an increased level of CD40L expression on Th cells and a greater number of cells expressing CD40L. Studies have documented the disregulated expression of CD40L on Th cells in SNF_1 mice (16) as well as in lupus patients (27), whereby autoreactive Th cells of lupus express an abnormally high level of CD40L, including T cells taken directly from patients without further in vitro stimulation. CD40L has also been shown to be expressed on normal human B cells when stimulated in vitro and, surprisingly, B cells from lupus patients have been found to exhibit endogenous hyperexpression of CD40L, reaching the level expressed by activated Th cells (27, 28). (It should be noted that we have examined both freshly isolated and mitogen-stimulated purified B cells from SNF_1 mice at various ages and have been unable to convincingly detect CD40L either by flow cytometry or RT-PCR (data not shown)). Interestingly, previous examination of freshly isolated PBMCs from lupus patients has shown that patients with the highest level of CD40L expression had active or end stage renal disease (28). Lastly, with advanced disease, it is possible that non-T, CD40L-bearing cells, as found in humans, such as stimulated NK cells (29), vascular endothelial cells, smooth muscle cells, and macrophages (30) may interact with and activate $CD40^+$ cells, resulting in an expanded pool of stimulated lymphoid and non-lymphoid cells.

Together the above data indicate that interrupting CD40-CD40L interaction not only blocks the initiation and maintenance of the pathogenic immune response, particularly the humoral arm of the response, but is also beneficial during the effector phase of disease when CD40-CD40L interaction takes place in a T/non-B cell or non-T/non-B cell setting. Indeed, the presence of CD40 on vascular endothelial cells (31, 32) and on a variety of parenchymal and nonparenchymal cells in the normal human kidney has already been established (33). Interestingly, in patients with lupus nephritis, CD40 expression is markedly increased in the kidney along with the presence of infiltrating $CD40L^+$ mononuclear cells (33). Because CD40-mediated signals can induce secretion of proinflammatory cytokines by monocytes, dendritic cells, and fibroblasts (34–37), it has been suggested that $CD40L^+$ mononuclear cells may interact with $CD40^+$ renal target cells to induce or enhance proinflammatory molecules that contribute to renal inflammation and damage (33). van Kooten et al. (38) have recently demonstrated that cross-linking CD40 on human proximal tubular epithelial cells leads to the production of chemokines IL-8, monocyte chemoattractant protein (MCP)-1, and RANTES, known inflammatory mediators that may contribute to the pathway leading to tissue damage and fibrosis. RANTES may be of particular importance since it is a known chemoattractant for T cells (39), and IL-2 and IFN-γ produced by activated T cells can directly activate human proximal tubular epithelial cells (40–42), thus providing a positive feedback loop for interstitial infiltration. In fact, Lloyd et al. (43) have used a nephrotoxic serum animal model to show that MCP-1 is indeed involved in glomerular crescent formation and interstitial fibrosis and together with RANTES plays a role in the inflammatory phase of crescentic nephritis. The ability of anti-CD40L immunotherapy to inhibit the development of fibrosis is of special significance given that there is a correlation between the degree of interstitial fibrosis and incidence of chronic renal failure in patients with glomerular diseases (44, 45). Current studies are underway to examine CD40, CD40L, and chemokine expression in SNF_1 mice treated with anti-CD40L vs controls.

It has been suggested that anti-CD40L may not be effective after establishment of disease, particularly for Th1-mediated autoimmune diseases (46). Our report demonstrates that long-term immunotherapy with an anti-CD40L mAb provides significant therapeutic benefit to nephritic, autoimmune SNF_1 female mice, a lupus model in which the nephritogenic autoantibodies are Th1-dependent (47). Cytokines from CD40L-expressing Th2 cells have also been shown to be necessary for survival of autoimmune B cells and disease progression in lupus (48, 49); thus, our data suggest that preventing CD40-CD40L interaction has consequences for both the Th1 and Th2 subpopulations of T cells. Furthermore, we present the longest survival of SNF_1 females ever reported, which is extraordinary at age 15.5 mo. At this age these animals continued to appear in good health with no obvious signs of infection or complications, which is particularly remarkable given that they are autoimmune-prone and were housed in a conventional facility. Importantly, there was no effect on total serum Ig levels (data not shown) indicating there was no general immunosuppression. These data suggest that long-term immunotherapy with anti-CD40L in people may not result in significant detrimental consequences, and overall the data lend promise to the potential use of anti-CD40L immunotherapy to treat human SLE and, possibly, other autoimmune diseases as well.

Acknowledgments

We thank Joseph Amatucci for production and purification of the Ha4/8-3.1 mAb, Konrad Miatowski and Janine Ferrant for production and purification, respectively, of the anti-CD40L mAb, Arthur McAllister for statistical analysis, Dr. Fabienne Mackay for useful suggestions and technical advice regarding immunohistochemistry, and Drs. Yen-Ming Hsu and

Chris Benjamin for a critical reading of the manuscript and many thought-provoking discussions.

References

1. Boumpas, D. T., H. A. R. Austin, B. J. Fessler, J. E. Balow, J. H. Klippel, and M. D. Lockshin. 1995. Systemic lupus erythematosus: emerging concepts. Part 1: Renal, neuropsychiatric, cardiovascular, pulmonary, and hematologic disease. *Ann. Intern. Med. 122:940.*
2. Datta, S. K., H. Patel, and D. Berry. 1987. Induction of a cationic shift in IgG anti-DNA autoantibodies: role of T helper cells with classical and novel phenotypes in three murine models of lupus nephritis. *J. Exp. Med. 165:1252.*
3. Shivakumar, S., G. C. Tsokos, and S. K. Datta. 1989. T cell receptor alpha/beta-expressing double-negative ($CD4^-/CD8^-$) and $CD4^+$ T helper cells in humans augment the production of pathogenic anti-DNA autoantibodies associated with lupus nephritis. *J. Immunol. 143:103.*
4. Mohan, C., S. Adams, V. Stanik, and S. K. Datta. 1993. Nucleosome: a major immunogen for pathogenic autoantibody-inducing T cells of lupus. *J. Exp. Med. 177:1367.*
5. Sainis, K., and S. K. Datta. 1988. $CD4^+$ T cell lines with selective patterns of autoreactivity as well as $CD4^-$ $CD8^-$ T helper cell lines augment the production of idiotypes shared by pathogenic anti-DNA autoantibodies in the NZB × SWR model of lupus nephritis. *J. Immunol. 140:2215.*
6. Adams, S., T. Zordan, K. Sainis, and S. Datta. 1990. T cell receptor V beta genes expressed by IgG anti-DNA autoantibody-inducing T cells in lupus nephritis: forbidden receptors and double-negative T cells. *Eur. J. Immunol. 20:1435.*
7. Ando, D. G., E. E. Sercarz, and B. H. Hahn. 1987. Mechanisms of T and B cell collaboration in the in vitro production of anti-DNA antibodies in the NZB/NZW F_1 murine SLE model. *J. Immunol. 138:3185.*
8. Rajagopalan, S., T. Zordan, G. C. Tsokos, and S. K. Datta. 1990. Pathogenic anti-DNA autoantibody-inducing T helper cell lines from patients with active lupus nephritis: isolation of $CD4^-8^-$ T helper cell lines that express the gamma delta T-cell antigen receptor. *Proc. Natl. Acad. Sci. USA 87:7020.*
9. Naiki, M., B. L. Chiang, D. Cawley, A. Ansari, S. J. Rozzo, B. L. Kotzin, A. Zlotnik, and M. E. Gershwin. 1992. Generation and characterization of cloned T helper cell lines for anti- DNA responses in NZB.H-2bm12 mice. *J. Immunol. 149:4109.*
10. Durie, F. H., T. M. Foy, S. R. Masters, J. D. Laman, and R. J. Noelle. 1994. The role of CD40 in the regulation of humoral and cell-mediated immunity. *Immunol. Today 15:406.*
11. Durie, F. H., R. A. Fava, T. M. Foy, A. Aruffo, J. A. Ledbetter, and R. J. Noelle. 1993. Prevention of collagen-induced arthritis with an antibody to gp39, the ligand for CD40. *Science 261:1328.*
12. Gerritse, K., J. D. Laman, R. J. Noelle, A. Aruffo, J. A. Ledbetter, W. J. Boersma, and E. Claassen. 1996. CD40-CD40 ligand interactions in experimental allergic encephalomyelitis and multiple sclerosis. *Proc. Natl. Acad. Sci. USA 93:2499.*
13. Griggs, N. D., S. S. Agersborg, R. J. Noelle, J. A. Ledbetter, P. S. Linsley, and K. S. Tung. 1996. The relative contribution of the CD28 and gp39 costimulatory pathways in the clonal expansion and pathogenic acquisition of self-reactive T cells. *J. Exp. Med. 183:801.*
14. Durie, F. H., A. Aruffo, J. Ledbetter, K. M. Crassi, W. R. Green, L. D. Fast, and R. J. Noelle. 1994. Antibody to the ligand of CD40, gp39, blocks the occurrence of the acute and chronic forms of graft-vs-host disease. *J. Clin. Invest. 94:1333.*
15. Blazar, B. R., P. A. Taylor, A. Panoskaltsis-Mortari, J. Buhlman, J. Xu, R. A. Flavell, R. Korngold, R. Noelle, and D. A. Vallera. 1997. Blockade of CD40 ligand-CD40 interaction impairs $CD4^+$ T cell-mediated alloreactivity by inhibiting mature donor T cell expansion and function after bone marrow transplantation. *J. Immunol. 158:29.*
16. Mohan, C., Y. Shi, J. D. Laman, and S. K. Datta. 1995. Interaction between CD40 and its ligand gp39 in the development of murine lupus nephritis. *J. Immunol. 154:1470.*
17. Early, G. S., W. Zhao, and C. M. Burns. 1996. Anti-CD40 ligand antibody treatment prevents the development of lupus-like nephritis in a subset of New Zealand black × New Zealand white mice: response correlates with the absence of an anti-antibody response. *J. Immunol. 157:3159.*
18. Noelle, R. J., M. Roy, D. M. Shepherd, I. Stamenkovic, J. A. Ledbetter, and A. Aruffo. 1992. A 39-kDa protein on activated helper T cells binds CD40 and transduces the signal for cognate activation of B cells. *Proc. Natl. Acad. Sci. USA 89:6550.*
19. Manaligod, J. R., C. L. Pirani, F. Miyasato, and V. E. Pollak. 1967. The renal changes in NZB/B1 and NZB-NZW F_1 hybrid mice: light and electron microscopic studies. *Nephron 4:215.*
20. Datta, S. K., P. J. McConahey, N. Manny, A. N. Theofilopoulos, F. J. Dixon, and R. S. Schwartz. 1978. Genetic studies of autoimmunity and retrovirus expression in crosses of New Zealand black mice. II. The viral envelope glycoprotein gp70. *J. Exp. Med. 147:872.*
21. Peto, R., M. C. Pike, P. Armitage, N. E. Breslow, D. R. Cox, S. V. Howard, N. Mantel, K. McPherson, J. Peto, and P. G. Smith. 1977. Design and analysis of randomized clinical trials requiring prolonged observation of each patient. II. Analysis and examples. *Br. J. Cancer 35:1.*
22. Strutz, F., and E. G. Neilson. 1994. The role of lymphocytes in the progression of interstitial disease. *Kidney Int. 45(Suppl.):S106.*
23. Okada, H., F. Strutz, T. M. Danoff, and E. G. Neilson. 1996. Possible pathogenesis of renal fibrosis. *Kidney Int. 54(Suppl.):S37.*
24. Eastcott, J. W., R. S. Schwartz, and S. K. Datta. 1983. Genetic analysis of the inheritance of B cell hyperactivity in relation to the development of autoantibodies and glomerulonephritis in NZB × SWR crosses. *J. Immunol. 131:2232.*
25. Lane, P., C. Burdet, F. McConnell, A. Lanzavecchia, and E. Padovan. 1995. CD40 ligand-independent B cell activation revealed by CD40 ligand-deficient T cell clones: evidence for distinct activation requirements for antibody formation and B cell proliferation. *Eur. J. Immunol. 25:1788.*
26. Ma, J., J. Xu, M. P. Madaio, Q. Peng, J. Zhang, I. S. Grewal, R. A. Flavell, and J. Craft. 1996. Autoimmune *lpr/lpr* mice deficient in CD40 ligand: spontaneous Ig class switching with dichotomy of autoantibody responses. *J. Immunol. 157:417.*
27. Desai-Mehta, A., L. Lu, R. Ramsey-Goldman, and S. K. Datta. 1996. Hyperexpression of CD40 ligand by B and T cells in human lupus and its role in pathogenic autoantibody production. *J. Clin. Invest. 97:2063.*
28. Koshy, M., D. Berger, and M. K. Crow. 1996. Increased expression of CD40 ligand on systemic lupus erythematosus lymphocytes. *J. Clin. Invest. 98:826.*
29. Carbone, E., G. Ruggiero, G. Terrazzano, C. Palomba, C. Manzo, S. Fontana, H. Spits, K. Karre, and S. Zappacosta. 1997. A new mechanism of NK cell cytotoxicity activation: the CD40-CD40 ligand interaction. *J. Exp. Med. 185:2053.*
30. Mach, F., U. Schonbeck, G. K. Sukhova, T. Bourcier, J. Y. Bonnefoy, J. S. Pober, and P. Libby. 1997. Functional CD40 ligand is expressed on human vascular endothelial cells, smooth muscle cells, and macrophages: implications for CD40-CD40 ligand signaling in atherosclerosis. *Proc. Natl. Acad. Sci. USA 94:1931.*
31. Hollenbaugh, D., N. Mischel-Petty, C. P. Edwards, J. C. Simon, R. W. Denfeld, P. A. Kiener, and A. Aruffo. 1995. Expression of functional CD40 by vascular endothelial cells. *J. Exp. Med. 182:33.*
32. Yellin, M. J., J. Brett, D. Baum, A. Matsushima, M. Szabolcs, D. Stern, and L. Chess. 1995. Functional interactions of T cells with endothelial cells: the role of CD40L-CD40-mediated signals. *J. Exp. Med. 182:1857.*
33. Yellin, M. J., V. D'Agati, G. Parkinson, A. S. Han, A. Szema, D. Baum, D. Estes, M. Szabolcs, and L. Chess. 1997. Immunohistologic analysis of renal CD40 and CD40L expression in lupus nephritis and other glomerulonephritides. *Arthritis Rheum. 40:124.*
34. Alderson, M. R., R. J. Armitage, T. W. Tough, L. Strockbine, W. C. Fanslow, and M. K. Spriggs. 1993. CD40 expression by human monocytes: regulation by cytokines and activation of monocytes by the ligand for CD40. *J. Exp. Med. 178:669.*
35. Caux, C., C. Massacrier, B. Vanbervliet, B. Dubois, C. Van Kooten, I. Durand, and J. Banchereau. 1994. Activation of human dendritic cells through CD40 cross-linking. *J. Exp. Med. 180:1263.*
36. Yellin, M. J., S. Winikoff, S. M. Fortune, D. Baum, M. K. Crow, S. Lederman, and L. Chess. 1995. Ligation of CD40 on fibroblasts induces CD54 (ICAM-1) and CD106 (VCAM- 1) up-regulation and IL-6 production and proliferation. *J. Leukocyte Biol. 58:209.*
37. Stout, R. D., J. Suttles, J. Xu, I. S. Grewal, and R. A. Flavell. 1996. Impaired T cell-mediated macrophage activation in CD40 ligand-deficient mice. *J. Immunol. 156:8.*
38. van Kooten, C., J. S. Gerritsma, M. E. Paape, L. A. van Es, J. Banchereau, and M. R. Daha. 1997. Possible role for CD40-CD40L in the regulation of interstitial infiltration in the kidney. *Kidney Int. 51:711.*
39. Schall, T. J., K. Bacon, K. J. Toy, and D. V. Goeddel. 1990. Selective attraction of monocytes and T lymphocytes of the memory phenotype by cytokine RANTES. *Nature 347:669.*
40. Seelen, M. A., R. A. Brooimans, F. J. van der Woude, L. A. van Es, and M. R. Daha. 1993. IFN-gamma mediates stimulation of complement C4 biosynthesis in human proximal tubular epithelial cells. *Kidney Int. 44:50.*
41. Brooimans, R. A., A. P. Stegmann, W. T. van Dorp, A. A. van der Ark, F. J. van der Woude, L. A. van Es, and M. R. Daha. 1991. Interleukin 2 mediates stimulation of complement C3 biosynthesis in human proximal tubular epithelial cells. *J. Clin. Invest. 88:379.*
42. Gerritsma, J. S., A. F. Gerritsen, M. De Ley, L. A. van Es, and M. R. Daha. 1997. Interferon-gamma induces biosynthesis of complement components C2, C4 and factor H by human proximal tubular epithelial cells. *Cytokine 9:276.*
43. Lloyd, C. M., A. W. Minto, M. E. Dorf, A. Proudfoot, T. N. Wells, D. J. Salant, and J. C. Gutierrez-Ramos. 1997. RANTES and monocyte chemoattractant protein-1 (MCP-1) play an important role in the inflammatory phase of crescentic nephritis, but only MCP-1 is involved in crescent formation and interstitial fibrosis. *J. Exp. Med. 185:1371.*
44. Risdon, R. A., J. C. Sloper, and H. E. De Wardener. 1968. Relationship between renal function and histological changes found in renal-biopsy specimens from patients with persistent glomerular nephritis. *Lancet ii:363.*
45. Bohle, A., M. Wehrmann, O. Bogenschutz, C. Batz, W. Vogl, H. Schmitt, C. A. Muller, and G. A. Muller. 1992. The long-term prognosis of the primary glomerulonephritides: a morphological and clinical analysis of 1747 cases. *Pathol. Res. Pract. 188:908.*
46. Stuber, E., W. Strober, and M. Neurath. 1996. Blocking the CD40L-CD40 interaction in vivo specifically prevents the priming of T helper 1 cells through the inhibition of interleukin 12 secretion. *J. Exp. Med. 183:693.*
47. Kaliyaperumal, A., C. Mohan, W. Wu, and S. K. Datta. 1996. Nucleosomal peptide epitopes for nephritis-inducing T helper cells of murine lupus. *J. Exp. Med. 183:2459.*
48. Datta, S. K., A. Kaliyaperumal, and A. Desai-Mehta. 1997. T cells of lupus and molecular targets for immunotherapy. *J. Clin. Immunol. 17:11.*
49. Nakajima, A., S. Hirose, H. Yagita, and K. Okumura. 1997. Roles of IL-4 and IL-12 in the development of lupus in NZB/W F_1 mice. *J. Immunol. 158:1466.*

Attachment 4

Very Low-Dose Tolerance with Nucleosomal Peptides Controls Lupus and Induces Potent Regulatory T Cell Subsets[1,2]

Hee-Kap Kang,* Marissa A. Michaels,* Beate R. Berner,† and Syamal K. Datta[3]*

We induced very low-dose tolerance by injecting lupus prone (SWR × NZB)F_1 (SNF1) mice with 1 μg nucleosomal histone peptide autoepitopes s.c. every 2 wk. The subnanomolar peptide therapy diminished autoantibody levels and prolonged life span by delaying nephritis, especially by reducing inflammatory cell reaction and infiltration in kidneys. $H4_{71-94}$ was the most effective autoepitope. Low-dose tolerance therapy induced $CD8^+$, as well as $CD4^+CD25^+$ regulatory T (T_{reg}) cell subsets containing autoantigen-specific cells. These adaptive T_{reg} cells suppressed IFN-γ responses of pathogenic lupus T cells to nucleosomal epitopes at up to a 1:100 ratio and reduced autoantibody production up to 90–100% by inhibiting nucleosome-stimulated T cell help to nuclear autoantigen-specific B cells. Both $CD4^+CD25^+$ and $CD8^+$ T_{reg} cells produced and required TGF-β1 for immunosuppression, and were effective in suppressing lupus autoimmunity upon adoptive transfer in vivo. The $CD4^+CD25^+$ T cells were partially cell contact dependent, but $CD8^+$ T cells were contact independent. Thus, low-dose tolerance with highly conserved histone autoepitopes repairs a regulatory defect in systemic lupus erythematosus by generating long-lasting, TGF-β-producing T_{reg} cells, without causing allergic/anaphylactic reactions or generalized immunosuppression. ***The Journal of Immunology,*** **2005, 174: 3247–3255.**

Nucleosomes, derived from apoptotic cells (1), are major immunogens for initiating cognate interactions between autoimmune Th and B cells in systemic lupus erythematosus (SLE)[4] (2). $CD4^+$ Th cells drive the production of pathogenic anti-DNA autoantibodies in lupus patients and lupus-prone SNF1 mice (3, 4). Only certain peptides in nucleosomal histones are immunodominant, and spontaneous priming to these particular epitopes occurs in preclinical lupus. The five major autoepitopes for lupus nephritis-inducing Th cells in murine and human lupus are $H1'_{22-42}$, $H2B_{10-33}$, $H3_{85-102}$, $H4_{16-39}$, and $H4_{71-94}$ (5–7). These peptide epitopes are cross-reactively recognized by autoimmune Th cells and B cells. The peptides accelerate lupus nephritis upon immunization, but they delay or even reverse disease upon tolerization in high doses (5, 6, 8). These nucleosomal peptides can be promiscuously presented and recognized in the context of diverse MHC class II alleles, behaving like universal epitopes (9, 10). Thus, universally tolerogenic peptides could be developed for therapy of lupus in humans despite their HLA diversity. High-dose tolerance therapy (300 μg i.v.) with the autoepitopes was effective in halting the progression of established lupus nephritis in SNF1 mice (8). However, high-dose peptide given i.v. may not be suitable in humans. Therefore, in this study, we developed therapy with 300-fold lower doses of the epitopes administrated s.c.

Materials and Methods

Mice

NZB and SWR mice were purchased from The Jackson Laboratory. Lupus-prone SNF1 hybrids were bred and females were used, as approved by the Animal Care and Use Committee.

Peptides

All peptides were synthesized by F-moc chemistry and their purity was checked by amino acid analysis by the manufacturer (Chiron Mimotopes).

Tolerance induction with very low doses of peptides

For long-term experiments, serologically autoimmune, but prenephritic, 12-wk-old SNF1 females (nine mice per group) were injected s.c. with either $H1'_{22-42}$, $H2B_{10-33}$, $H2B_{59-73}$, $H4_{16-39}$, or $H4_{71-94}$ peptide (1 μg/mouse) in saline every 2 wk until the animals died. Control group received only saline. The mice were monitored weekly for proteinurea using albustix (VWR Scientific). Sera were collected every 2½ months for the determination of total IgG and IgG subclasses of antinuclear autoantibodies. A parallel batch of identically treated mice of each group was followed and sacrificed at different time points for evaluation of renal lesions. To test the immunological consequences of the tolerance therapy early on, another batch of 12-wk-old SNF1 mice (five per group) were treated as above, but they received a total of three injections of each peptide at 2-wk intervals. Ten days after the third injection, these short-term batches of mice were sacrificed for analysis of autoimmune T and B cells and regulatory T (T_{reg}) cells.

Autoantibody quantitation

IgG class autoantibodies to ssDNA, dsDNA, histone and nucleosome (histone-DNA complex) were measured by ELISA (2, 6). Subclasses of IgG autoantibodies were detected by ELISA using alkaline phosphatase (AP)-conjugated anti-mouse IgG1, IgG2a, IgG2b, and IgG3 (Southern Biotechology Associates).

Cell isolation

Total, $CD4^+$ and $CD8^+$ T cells from spleens were purified by appropriate MACS isolation kits using magnetic bead-conjugated Abs specific to each

*Departments of Medicine and Microbiology-Immunology, Division of Rheumatology, Northwestern University Feinberg School of Medicine, Chicago, IL 60611; and †Department of Pathology, Case Western Reserve University, Cleveland, OH 44106

Received for publication November 8, 2004. Accepted for publication January 3, 2005.

The costs of publication of this article were defrayed in part by the payment of page charges. This article must therefore be hereby marked *advertisement* in accordance with 18 U.S.C. Section 1734 solely to indicate this fact.

[1] This work was supported by National Institutes of Health Grants R37-AR39157 and RO1-AI41985 (to S.K.D.).

[2] Preliminary results on low-dose peptide tolerance were presented by us as an abstract at the Annual Meeting of American College of Rheumatology in 2002 (Arthritis Rheum. 46, Supplement: S225, Abstract 526, 2002).

[3] Address correspondence and reprint requests to Dr. Syamal K. Datta, Division of Rheumatology, Northwestern University Feinberg School of Medicine, 240 East Huron Street, McGaw 2300, Chicago, IL 60611. E-mail address: skd257@northwestern.edu

[4] Abbreviations used in this paper: SLE, systemic lupus erythematosus; T_{reg}, regulatory T; HEL, hen egg lysozyme; AP, alkaline phosphatase; GITR, glucocorticoid-induced TNFR family-related protein; PAS, periodic acid-Schiff.

0022-1767/05/$02.00

Ag. $CD4^+CD25^+$ T cells were purified by a mouse regulatory T cell isolation kit according to the manufacturer's protocol (Miltenyi Biotec). $CD28^+$ and $CD28^-$ subsets of $CD8^+$ T cells were separated by using anti-CD28-PE conjugate and anti-PE Microbeads (Miltenyi Biotec). Purity of all isolated cell subsets was >90%.

Adoptive transfer

$CD4^+CD25^-$, $CD4^+CD25^+$, or $CD8^+$ T cells (1×10^6 cells/mouse) from low-dose peptide ($H4_{71-94}$ or $H4_{16-39}$)-tolerized SNF1 mice were purified by MACS and then immediately injected i.v. into 4-mo-old SNF1 mice. One day after transfer, the mice were immunized i.p. with 100 μg of $H1'_{22-42}$ peptide in CFA, which accelerates lupus nephritis. Recipient mice were monitored for nephritis and IgG autoantibody levels in serum.

ELISPOT assay

ELISPOT assay plates (Cellular Technology) were coated with capture Abs against IL-2, IL-4, IL-10, or IFN-γ (BD Pharmingen) in PBS at 4°C overnight. Splenic T cells (1×10^6) from treated mice were cultured with irradiated (3000 rad) splenic APC (B cells, macrophages, and dendritic cells) from 1-mo-old SNF1 mice in the presence of peptides or PBS alone as control. Cells were removed after 24 h of incubation for IFN-γ and IL-2 or 48 h for IL-4 and IL-10, and the reactions were visualized by addition of the individual anti-cytokine Ab-biotin and subsequent AP-conjugated streptavidin. Cytokine-expressing cells were detected by Immunospot scanning and analysis (Cellular Technology).

Cytokine ELISA

$CD4^+$ T cells (1×10^6) or $CD8^+$ T cells (1×10^6) from low-dose peptide-tolerized or -unmanipulated SNF1 mice were stimulated with $H4_{71-94}$ peptide or Ab to CD3 (1 μg/ml) with splenic APC. Culture supernatants were collected after 48 h (for TGF-β1, after 72 h). IL-10 was measured by BD OptEIA ELISA set (BD Pharmingen). For TGF-β1, samples were acidified by addition of HCl at 20 mM for 15 min and neutralized by NaOH, and then amounts of TGF-β1 were measured by a TGF-β1 Emax Immuno-Assay System (Promega).

Helper suppression assay

To detect suppression of autoantibody-inducing help, whole T cells (2.5×10^6/well) or purified $CD4^+CD25^-$, $CD4^+CD25^+$, or $CD8^+$ T cells (0.3, 0.6, 1.25, or 2.5×10^6/well) from peptide-tolerized or saline-treated mice were cocultured with a helper assay mixture (6) consisting of splenic B cells (5×10^6/well) and Th cells (2.5×10^6/well) from 3- to 5-mo-old, unmanipulated SNF1 mice in 24-well plates (or in 96-well plates with 1/10 cell numbers) for 7 days. The cocultures were performed in the presence of 10 μg/ml cognate peptides or 1 μg/ml nucleosomes. Culture supernatants were collected and assayed for IgG Abs against dsDNA, ssDNA, histones, and nucleosomes as described elsewhere (6). Helper suppression assays were also performed in the presence of anti-IL-10 Ab (10–250 μg/ml), anti-TGF-β Ab (10–250 μg/ml), or isotype control for each (R&D Systems) (11).

Transwell experiments

T_{reg} cells (7.5×10^5) from peptide-treated SNF1 mice plus APC (7.5×10^5) were placed in Transwell chambers (12) separated by a 0.4-μm permeable membrane (Corning Costar) from a helper assay coculture of splenic B cells (7.5×10^5/well) from 4- to 5-mo old and T cells (7.5×10^5/well) from 3- to 4-mo-old unmanipulated SNF1 mice. After 7 days of culture, supernatants were assayed for IgG autoantibodies.

Flow cytometry

T cells from tolerized or control mice were stained with PE-conjugated anti-CD62L, CTLA-4, CD69, PD-1, or 4-1BB (BD Pharmingen), TGF-β1, latency-associated protein, or glucocorticoid-induced TNFR family related gene (GITR; R&D Systems) at 4°C for 30 min, as described previously (13, 14). Matched PE-conjugated IgG isotype controls were used. Cells were then stained with FITC-conjugated anti-CD25 and CyChrome-conjugated anti-CD4 at 4°C for 20 min. For intracellular CTLA-4 staining, cells were first surface-labeled with FITC-conjugated anti-CD25 and Cy-conjugated anti-CD4 for 20 min at 4°C. Cells were then fixed and permeabilized and then stained with PE-anti-CTLA-4 or PE-IgG isotype control. Cells were analyzed using FACSCalibur (BD Pharmingen).

Real-time RT-PCR

RNA from T cell subsets was isolated by RNeasy kit (Qiagen) and then cDNA synthesized to measure expression of Foxp3, as described previously (15).

Examination of kidneys

Kidney sections were stained with H&E and periodic acid-Schiff and graded 0–4+ for pathologic changes in a blinded fashion, as described elsewhere (6, 8, 16, 17). Immunohistochemistry was done as previously described (6, 17).

ELISA for anti-hen egg lysozyme (HEL) Abs

HEL (10 μg/ml) was coated onto 96-well plates (Nunc). After blocking with 1% BSA in PBS, serially diluted sera were added. Anti-HEL IgG Abs were detected by AP-conjugated anti-mouse IgG (Southern Biotechnology Associates).

Statistical analysis

Chi-square test, log rank test, and the Student two-tailed t test were used. Results are expressed as mean ± SEM.

Results

Very low-dose peptide epitope therapy postpones lupus nephritis and prolongs life span

Twelve-weel-old prenephritic SNF1 females (nine mice per group) were injected s.c. every 2 wk with one of the major autoepitopes, $H1'_{22-42}$, $H2B_{10-33}$, $H4_{16-39}$, or $H4_{71-91}$, or a nonstimulatory peptide $H2B_{59-73}$, each at 1 μg (~0.42 nM) of peptide per dose per mouse in saline. A control group received only saline. The control group started developing severe nephritis from 20 wk of age, as documented by persistent proteinurea of >100 mg/dl, and a 3–4+ renal pathology (Fig. 1*A*). At 31 wk of age, 60% of the saline control group, 40% of the $H2B_{59-73}$ peptide-injected group, and 33.3% of the $H2B_{10-33}$-injected group of mice developed severe nephritis ($p > 0.2$), whereas the $H1'_{22-42}$, $H4_{16-39}$, or $H4_{71-94}$ peptide-injected mice did not develop disease at this time point ($p < 0.01$). The largest differences were at 35–38 wk of age, when 80% of the control mice had severe nephritis and the $H2B_{10-33}$, $H2B_{59-73}$, or $H4_{16-39}$ group had an incidence of 44.4, 60, or 40%, respectively ($p > 0.1$–>0.2); whereas in the $H1'_{22-42}$ or $H4_{71-94}$ group the incidence was nil ($p < 0.01$). By 47 wk of age, all mice in the saline control group, 88.8% of the $H2B_{10-33}$ group, 80% of the $H2B_{59-73}$ group, and 85.7% of the $H4_{16-39}$ group developed severe nephritis, whereas only 40% of the $H1'_{22-42}$ ($p < 0.05$) and 20% of the $H4_{71-94}$ peptide-injected groups had severe nephritis ($p < 0.01$).

The saline-injected mice rapidly died within 12 mo (Fig. 1*B*). At this time, 22.2% of the $H2B_{10-33}$ and 20% of the $H2B_{59-73}$ peptide-treated animals were alive ($p > 0.2$), whereas 57.1% of the $H4_{16-39}$-treated ($p < 0.05$) and 100% of the $H1'_{22-42}$ and $H4_{71-94}$-treated animals were alive ($p < 0.01$). At 15 mo, 11.1% of $H2B_{10-33}$ and 20% of $H2B_{59-73}$-treated mice were alive ($p > 0.2$), whereas 42.9% of $H4_{16-39}$ ($p < 0.05$), 60% of $H1'_{22-42}$ ($p < 0.05$), and 100% of $H4_{71-94}$ ($p < 0.01$)-treated mice were alive. At 21 mo of age, 60% of $H4_{71-94}$ peptide-treated animals were alive ($p < 0.05$), whereas only 20% of $H1'_{22-42}$ and 33.3% of $H4_{16-39}$-treated mice were alive; but all other groups were dead. Therefore, very low-dose therapy with $H4_{71-94}$ extended the life span longer than 21 mo, in contrast to the control group that all died within 12 mo. Log rank test for survival was consistent: $H1'_{22-42}$-treated group ($p = 0.000315$), $H2B_{10-33}$-treated group ($p = 0.153$), $H2B_{59-73}$-treated group ($p = 0.217$), $H4_{16-39}$-treated ($p = 0.0162$), and $H4_{71-94}$-treated group ($p = 0.0000182$).

Three months after the start of therapy, kidney sections from control mice had an overall score of 3.5 ± 0.5 for nephritis, whereas the $H4_{71-94}$-, $H1'_{22-42}$-, or $H4_{16-39}$-treated groups showed 1.4 ± 0.8 as the overall score ($p < 0.001$; Fig. 1*C*). Glomerular IgG deposits were observed in kidneys from both tolerized and control mice (Fig. 1D), but perivascular and interstitial infiltrations of mononuclear cells containing $CD4^+$ and $CD8^+$ T cells

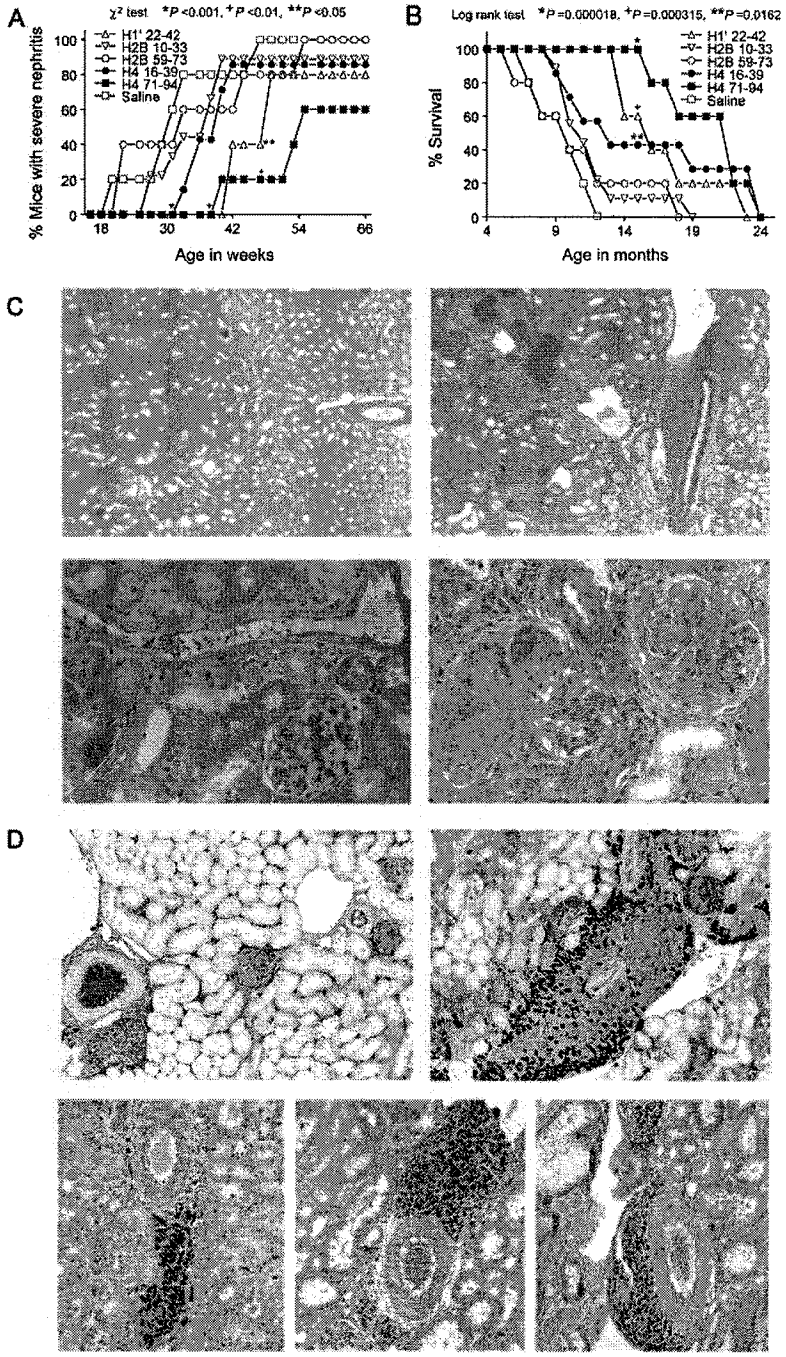

FIGURE 1. Beneficial effects of low-dose tolerance therapy. Incidence of severe lupus nephritis (*A*) and percent survival (*B*) of lupus-prone SNF1 mice injected with respective nucleosomal histone peptide or saline every 2 wk (nine mice/group). *C*, Representative kidney sections from peptide-tolerized (*left*, $H4_{71-94}$ peptide-treated in this example) or control (*right*, saline-treated) SNF1 mice (H&E; original magnification, ×100). The saline control shows marked perivascular and interstitial infiltrate of mononuclear cells, dilated tubules with casts, and hyalinized, sclerotic glomeruli. *Lower panels* (original magnification, ×400) show that in contrast to the peptide-treated mice (*left*), kidney from control-treated mice (*right*) shows advanced glomerular lesions with sclerosis, crescent formation, and marked thickening of basement membranes, and perivascular, interstitial infiltrates of mononuclear cells. *D*, Representative immunohistochemistry (original magnification, ×200) shows IgG deposits in glomeruli from both control (*right upper panel*) and peptide-tolerized (*left upper*) SNF1 mice. However, marked perivascular cellular infiltrates containing IgG^+ plasma cells (*upper right panel*), as well as $CD4^+$ T (*lower left panel*), $CD8^+$ T (*lower middle panel*), and $CD138^+$ plasma cells (*lower right panel*) were detected only in kidneys of control-treated mice as shown. Positive staining is brown. The results in *C* and *D* are representative of five mice per group.

and IgG-producing B cells were markedly reduced in the peptide-treated mice ($p < 0.001$).

Very low-dose peptide therapy reduces antinuclear autoantibody levels in serum

Sera were first assayed 2 wk after the fifth injection, i.e., 3 mo after starting therapy (at early nephritic age). $H4_{71-94}$ treatment, as compared with $H2B_{59-73}$ (Fig. 2*A*), was very effective in reducing levels of autoantibodies pathognomonic of lupus nephritis (18, 19). $H4_{71-94}$ therapy reduced IgG class autoantibodies to dsDNA, ssDNA, nucleosomes, and histones by 41.5, 50, 94.2, and 98.6%, respectively ($p < 0.01$, $p < 0.001$, $p < 0.001$, and $p < 0.001$, respectively); that of IgG2a subclass autoantibodies by 54, 95.3, 94, and 98%, respectively ($p < 0.01$, $p < 0.001$, $p < 0.001$, and $p < 0.001$, respectively); that of IgG2b autoantibodies by 82.9, 68, 89, and 88%, respectively ($p < 0.01$, $p < 0.01$, $p < 0.02$, and $p < 0.001$, respectively); and that of IgG3 autoantibodies by 45, 83.2, 80, and 99%, respectively (all $p < 0.001$). IgG1 autoantibody levels were already very low in the controls.

$H4_{16-39}$ therapy also reduced IgG autoantibodies to nuclear autoantigens as much as $H4_{71-94}$. $H1'_{22-42}$ therapy reduced the levels of IgG autoantibodies against dsDNA, ssDNA, and nucleosome effectively, but not against histone. $H2B_{10-33}$ reduced the levels of IgG2a autoantibodies against dsDNA and ssDNA by 25% ($p < 0.02$) and 85% ($p < 0.001$), respectively, and that of IgG2b autoantibodies against dsDNA, ssDNA, and nucleosomes by 93, 61, and 82%, respectively ($p < 0.001$, $p < 0.001$, and $p < 0.05$, respectively), but the levels of IgG2a against nucleosome and

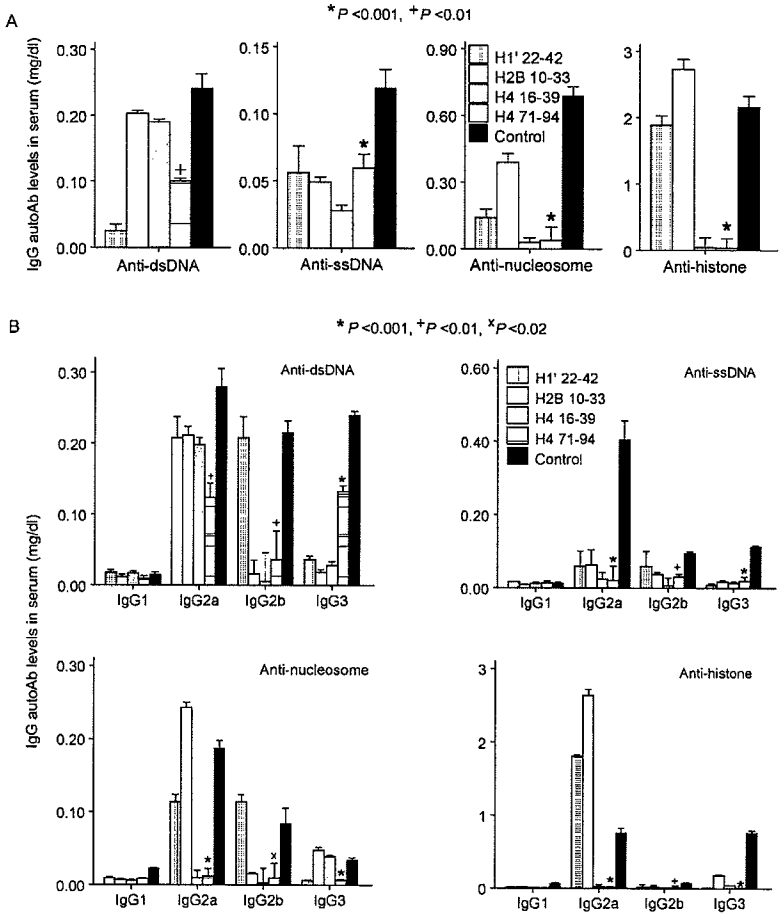

FIGURE 2. Low-dose peptide therapy markedly reduces the levels of IgG class autoantibodies (*A*) and their subclasses (*B*) in serum. In this sampling, SNF1 mice were bled after 3 mo of treatment (at 6 mo of age) and were assayed for levels of IgG autoantibodies to dsDNA, ssDNA, histone, and nucleosomes. Autoantibody levels (mean ± SEM, mg/dl) are from nine mice per treatment group (key within figure). It should be noted that the commercial Ab reagents used to measure IgG class as a whole vs IgG subclasses were different in sensitivity, thus the standard curves were not comparable.

histone actually increased by 29 and 34%, respectively. The low-dose peptide therapy did not cause IgG1 isotype shift (Th2 deviation), and total polyclonal IgG levels were not significantly different among the groups.

T cell response to autoepitopes was markedly reduced in peptide-treated mice

To test the immunologic consequences of the low-dose peptide therapy early on, a separate set of 12- to 14-wk-old SNF1 mice was injected with the most effective peptide epitope ($H4_{16-39}$ or $H4_{71-94}$), or saline, or $H2B_{59-73}$ every 2 wk, three times, and then sacrificed. Animals were 18–20 wk old at this time. T cells in unmanipulated SNF1 mice are spontaneously primed to the major nucleosomal peptide epitopes early in life and respond to them in vitro (5, 6). T cells from peptide-treated or control mice in this study were challenged with the epitopes by coculturing with APC in the presence of the peptides or nucleosomes, and their cytokine responses were measured (IL-2, IL-4, IL-10, and IFN-γ). Only IFN-γ was detected. T cells from $H1'_{22-42}$, $H4_{16-39}$, and $H4_{71-94}$-treated mice showed markedly reduced responses, as compared with the control group (Fig. 3*A*). $H1'_{22-42}$-treated mice showed the highest reduction at 1 μg/ml cognate epitope ($p < 0.001$). The therapy also reduced responses to other epitopes ($H4_{16-39}$, $H4_{71-94}$) cross-reactively ($p < 0.05$). $H4_{71-94}$ treatment resulted in the highest inhibition of response to cognate epitope at 0.1 μg/ml ($p < 0.01$), as well as to the other epitopes, $H1'_{22-42}$ and $H4_{16-39}$ ($p < 0.01$; Fig. 3*A*). $H4_{16-39}$ treatment also markedly reduced responses to cognate epitope (optimally at 1 μg/ml, $p < 0.001$) as well as to $H1'_{22-42}$ and $H4_{71-94}$ ($p < 0.001$).

Because low-dose peptide treatment reduced IFN-γ responses against histone peptide epitopes cross-reactively (Fig. 3*A*), T cell responses to whole nucleosomes were also assessed and found to be significantly reduced in $H4_{71-94}$-treated mice (Fig. 3*B*). Similar results were found in $H1'_{22-42}$ ($p < 0.01$) and $H4_{16-39}$-treated mice ($p < 0.001$, data not shown).

Very low-dose peptide therapy generates $CD8^+$ and $CD4^+CD25^+$ T_{reg} cells

Low-dose peptide treatment suppressed autoantibodies without causing Th1/Th2 deviation, indicating the possibility of T_{reg} cell involvement. Using the helper-suppression assay, the ability of $CD4^+CD25^-$ T cells, $CD4^+CD25^+$ T cells, or $CD8^+$ T cells from the peptide-treated mice to suppress nucleosome-stimulated autoantibody production in cocultures of lupus Th and B cells of unmanipulated SNF1 mice was determined. $CD4^+CD25^+$ T cells and $CD8^+$ T cells from tolerized mice strongly suppressed the ability of unmanipulated lupus $CD4^+$ T cells to help B cells to produce IgG autoantibodies (Fig. 4*A*). Because help was already optimal in the nucleosome-stimulated helper assay cultures, the levels of autoantibodies produced by unmanipulated SNF1 lupus Th and B cells cultured by themselves did not change significantly upon their cocultures with the $CD4^+CD25^-$ T cells from the treated mice. Compared with those levels, suppressions of autoantibodies to dsDNA, ssDNA, and nucleosomes by $CD4^+CD25^+$ T cells from $H4_{16-39}$-treated mice were 25, 98.8, and 83%, respectively ($p < 0.05$, $p < 0.001$, $p < 0.001$, respectively); from $H4_{71-94}$-treated were mice 24, 74, and 76% (all $p <$ 0.01–<0.001); but from age-matched unmanipulated SNF1 mice

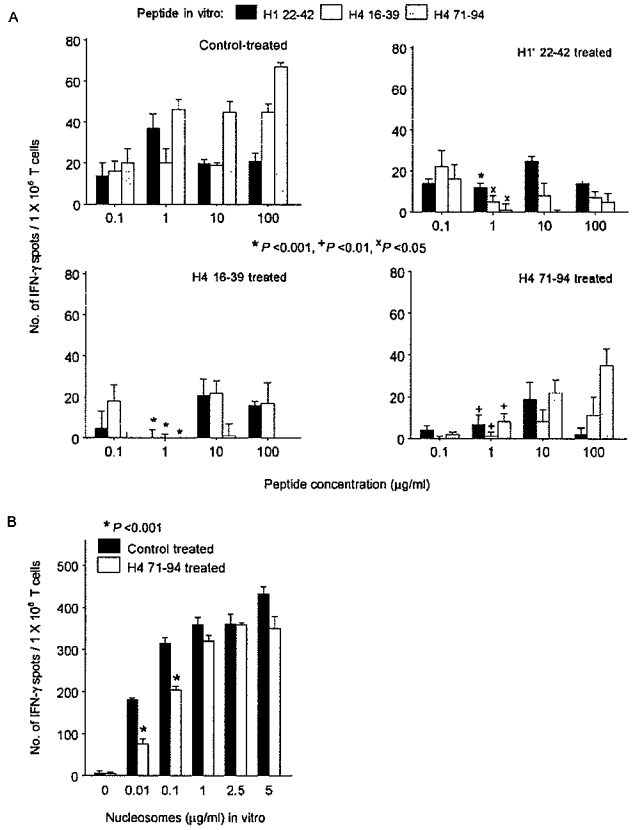

FIGURE 3. Low-dose peptide therapy decreases IFN-γ responses by lupus T cells in ELISPOT. *A*, Splenic T cells from saline, $H1'_{22-42}$, $H4_{16-39}$, or $H4_{71-94}$ peptide-treated SNF1 mice were challenged with tolerizing peptide epitope and other relevant epitopes in various concentrations in vitro. Baseline IFN-γ spots in lupus T plus APC cultures without Ag were 5 $\pm$ 3 spots per 1 $\times$ 10^6 T cells. *B*, Low-dose treatment with peptide ($H4_{71-94}$-treated group shown here) also inhibited IFN-γ responses to nucleosomes in vitro as compared with control SNF1 mice. IFN-γ responses are expressed in mean $\pm$ SEM positive spots per 1 $\times$ 10^6 T cells from three experiments (five mice per group).

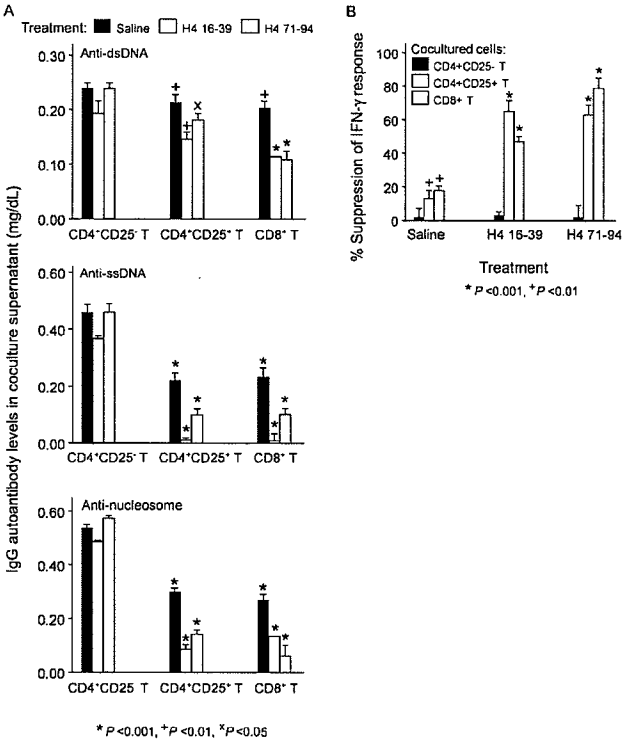

FIGURE 4. Induction of potent $CD4^+CD25^+$ and $CD8^+$ T_{reg} cells by low-dose peptide therapy. *A*, $CD4^+CD25^+$T cells and $CD8^+$ T cells from low-dose peptide-tolerized SNF1 mice suppressed anti-dsDNA, anti-ssDNA, and anti-nucleosome autoantibody production by lupus Th and B cells from 5-mo-old, unmanipulated SNF1 mice in the nucleosome-stimulated, helper suppression assay (in these examples, the ratio of T_{reg}:lupus Th was 1:1). Baseline levels of IgG autoantibodies produced by B cells cultured by themselves were: anti-dsDNA, 0.01 $\pm$ 0.005; anti-ssDNA, 0.04 $\pm$ 0.006; antinucleosome, 0.02 $\pm$ 0.001; and antihistone, 0.03 $\pm$ 0.002 mg/dl. *B*, T_{reg} cells induced by peptide treatment also suppressed directly the IFN-γ responses of unmanipulated SNF1 lupus T cells to nucleosomes presented by APC in the ELISPOT assay (ratio of T_{reg}:lupus Th = 1:10). Results are expressed as percent suppression (mean $\pm$ SEM) from three experiments (five mice per group). Baseline number of IFN-γ spots produced by lupus T cells plus APC cultures without Ag were 10 $\pm$ 4 spots per 1 $\times$ 10^6 T cells. The purity of each subset of T cells was >90%.

were 7, 6.2, and 17% ($p > 0.2$), respectively. Similarly, suppressions of autoantibody production to dsDNA, ssDNA, and nucleosome by $CD8^+$ T cells from the same groups, respectively, were 41, 99.8, and 72.6% (all $p < 0.001$); 55, 78,, and 90% (all $p < 0.001$); and 15, 17, and 21.2% ($p < 0.02$). Both sets of T_{reg} cells from peptide-treated mice were effective at up to a 1:10 ratio in inhibiting autoantibody production in the helper-suppression assays (data not shown).

Direct suppressing ability of the IFN-γ response to autoantigen was also determined by coculturing T_{reg} cells from treated mice with T cells from 5½-mo-old unmanipulated SNF1 mice in the presence of nucleosomes (1 μg/ml; Fig. 4*B*). Both sets of T_{reg} cells from peptide-treated mice were effective at up to a 1:100 ratio (T_{reg} cells:target lupus T cells) in strongly inhibiting autoantigen-specific responses of lupus T cells in ELISPOT assays ($p < 0.001$, Fig. 4*B*).

Taken together, $CD4^+CD25^+$ or $CD8^+$ T cells from peptide-treated mice showed 3- to 16-fold greater suppressive activity on autoantibody production and nucleosome-specific responses than equivalent numbers of those cells from age-matched control SNF1 mice (Fig. 4, $p < 0.01$–<0.001). Furthermore, we could not detect any differences in the suppressive ability of $CD28^+$ vs $CD28^-$ subsets of $CD8^+$ T cells, as found in other systems (20).

Adoptively transferred T_{reg} cells suppress autoantibody production and nephritis in vivo

We isolated each T_{reg} subset from peptide-treated mice and adoptively transferred them into prenephritic (4-mo-old) SNF1 mice. One day after adoptive cell transfer, recipient SNF1 mice were immunized with pathogenic $H1'_{22-42}$ in CFA. SNF1 mice immunized with $H1'_{22-42}$ (100 μg/mouse) in adjuvant (CFA) developed severe nephritis and produced high levels of autoantibodies earlier than age-matched SNF1 mice injected with CFA alone or the nonstimulatory peptide $H2B_{59-73}$ in CFA, as described previously (6). $CD4^+CD25^-$ T cell transfer did not affect autoantibody levels in the $H1'_{22-42}$-immunized mice, since they were maximally immunostimulated by autoantigen immunization (6). In comparison to those levels, suppression of serum autoantibodies to dsDNA, ssDNA, nucleosomes, and histone by $CD4^+CD25^+$ T_{reg} cells from $H4_{71-94}$-treated mice was 40, 75, 94, and 97%, respectively ($p <$ 0.025–$<$0.001) and from $H4_{16-39}$- treated mice was100, 80, 92, and 94%, respectively (all $p < 0.001$; Fig. 5). Suppression of the same IgG autoantibodies by $CD8^+$ T_{reg} cells from $H4_{71-94}$-treated group was 45, 95, 94, and 97%, respectively ($p <$ 0.025–$<$0.001)

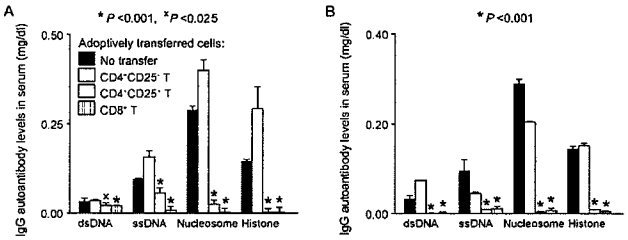

FIGURE 5. Adoptive transfer of T_{reg} cells suppresses pathogenic autoantibodies in lupus-accelerated SNF1 mice. $CD4^+CD25^-$ T, $CD4^+CD25^+$ T, and $CD8^+$ T cells from $H4_{71-94}$-treated (*A*) or $H4_{16-39}$-treated (**B**) SNF1 mice were purified by MACS and immediately injected i.v. into 16-wk-old recipient SNF1 at 1×10^6 cells/mouse. One day after transfer, the recipient mice were immunized with 100 μg of $H1'_{22-42}$ peptide in 0.1 ml of CFA. After transfer, proteinurea was measured every week. One month after immunization, sera were collected for measuring IgG class autoantibodies to nuclear Ags (five mice per group). Levels of autoantibodies in serum of $H1'_{22-42}$-immunized SNF1 mice without adoptive transfer were not significantly different from those in $H1'_{22-42}$-immunized SNF1 mice that had received $CD4^+CD25^-$ T cells from peptide-tolerized mice ($p > 0.05$). The purity of each subset of T cells was >90%.

and from $H4_{16-39}$-treated mice was 99, 76, 97, and 97%, respectively (all $p < 0.001$; Fig. 5). Both types of T_{reg} cells inhibited serum autoantibody levels for up to 2 mo after the one-time adoptive transfer. During this period, 30% of the $CD4^+CD25^-$ T cell recipient group developed severe nephritis within 6 wk of immunization with $H1'_{22-42}$ and died a week later (data not shown), whereas the incidence of severe nephritis and death in the T_{reg} cell recipient groups was nil at this time ($p < 0.05$). Because the lupus-prone mice were maximally stimulated by major autoepitope immunization, incidence of disease and level of autoantibodies in $H1'_{22-42}$-immunized SNF1 mice without adoptive transfer were not significantly different from that in $H1'_{22-42}$-immunized SNF1 mice that had received $CD4^+CD25^-$ T cells from peptide-tolerized mice (Fig. 5). After 2½ mo posttransfer, all of the mice receiving $CD4^+CD25^+$ T_{reg} cells still survived ($p < 0.05$), but 30% of mice receiving either $CD4^+CD25^-$ or $CD8^+$ cells were dead. The one-time recipients of $CD4^+CD25^+$ T_{reg} cells still had higher survival at 3½ mo posttransfer, as compared with the latter groups (75% vs 50%).

Both sets of T_{reg} produce TGF-β, but only $CD4^+CD25^+$ T_{reg} cells are partially contact dependent

We found that Ab to IL-10 (10–250 μg/ml) did not abrogate the suppression by the T_{reg} cells in the helper-suppression assay (data not shown). With 10-250 μg/ml anti-TGF-β Ab, $CD4^+CD25^+$ T cell-mediated suppression of production of autoantibodies to dsDNA was not affected; however, that to ssDNA and nucleosomes was reduced, but not abrogated. However, the suppression by regulatory $CD8^+$ T cells in the same helper assay cultures was almost completely abrogated by anti-TGF-β Ab (Fig. 6*A*). Furthermore, $CD8^+$ T_{reg} cells could suppress autoantibody production across a Transwell membrane barrier (Fig. 6*B*), indicating that soluble TGF-β from these cells mediates the immunosuppression.

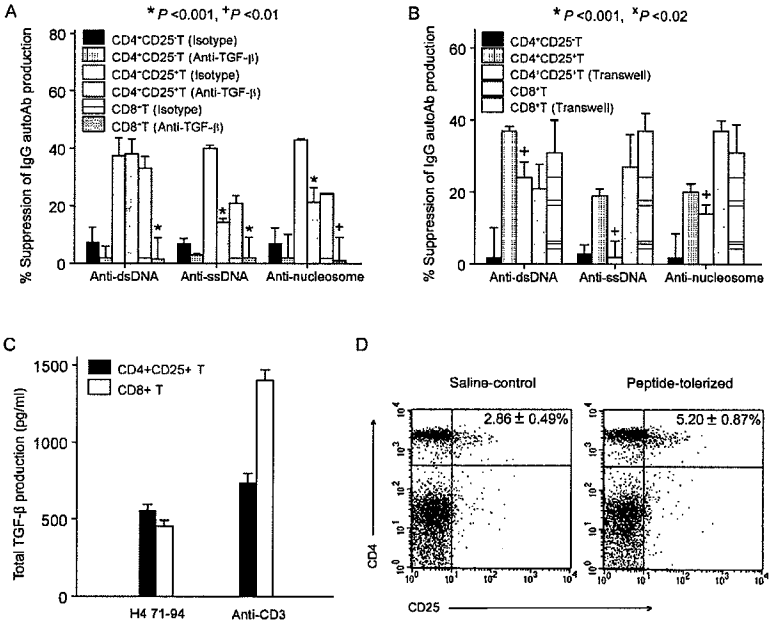

FIGURE 6. Suppression of IgG autoantibody production by $CD4^+CD25^+$ T cells is mediated by TGF-β and cell contact, but suppression by $CD8^+$ T cells is mediated mainly by TGF-β. $CD4^+CD25^+$ or $CD8^+$ T cells (5×10^5 each) from $H4_{71-94}$- or $H4_{16-39}$-tolerized mice were cocultured with T and B cells (1×10^6 each) from 3- to 4-mo-old unmanipulated SNF1mice in the presence of nucleosomes and anti-cytokine Abs (five mice per group). *A*, Representative helper suppression assay in the presence of 250 μg/ml anti-TGF-β or isotype control. *B*, T_{reg} cells were separated by membranes from helper assay mixtures containing nucleosomes plus lupus T and B cells from unmanipulated, 3- to 4-mo-old SNF1 in Transwell plates. It should be noted that the helper assay mixture of lupus T and B cells used here (*A* and *B*) came from 1- to 2-mo younger, unmanipulated SNF1 mice than those in Fig. 4*A*. The purity of each subtype of T cells was >90%. *C*, TGF-β1 production by $CD4^+CDC25^+$ or $CD8^+$ T cells (1×10^6 each) from $H4_{71-94}$ peptide-tolerized mice stimulated with $H4_{71-94}$ or soluble anti-CD3 (1 μg/ml) plus APC. Results are expressed in mean ± SEM from three experiments. Baseline values of TGF-β production without stimulation were 318 ± 14 pg/ml for $CD4^+CDC25^+$ T cells and 217 ± 20 pg/ml for $CD8^+$ T cells from the $H4_{71-94}$ peptide-tolerized mice. *D*, Percentage of $CD4^+CD25^+$ T cells in 1×10^6 splenocytes from low-dose peptide-tolerized mice and control mice are shown. This result is representative of nine separate experiments.

The $CD4^+CD25^+$ T cells showed reduced suppression of autoantibody production through the membrane, indicating their suppression is significantly contact dependent ($p < 0.01$). We next measured TGF-β1 production by T_{reg} cell subsets (Fig. 6*C*). Both $CD4^+CD25^+$ and $CD8^+$ T cells from peptide-treated mice produced increased amounts of total TGF-β1 upon stimulation with $H4_{71-94}$ or anti-CD3.

Phenotypes of $CD4^+CD25^+$ and $CD8^+$ T_{reg} cell subsets

We analyzed cell surface molecules that are relevant to T_{reg} cells (13, 14, 21). Peptide therapy increased the numbers of $CD4^+CD25^+$ T cells up to 1.8-fold more in SNF1 mice than in controls ($p < 0.02$; Fig. 6*D*). Total numbers of $CD4^+CD25^+$ $CD62L^+$ T cells per 1×10^6 splenocytes in peptide-tolerized mice were 2.3×10^4 and those from controls were 1.9-fold less (1.2×10^4). $CD4^+CD25^+$ cells, but not $CD8^+$ T_{reg} cells from $H4_{71-94}$- or $H4_{16-39}$-treated mice, showed slightly (1.3-fold) increased Foxp3 expression than controls ($p < 0.01$, data not shown). The $CD8^+$ T cell population was strongly positive for surface expression of TGF-β, CD62L, and GITR, and the $CD4^+CD25^+$ T cells were strongly positive for GITR, CD62L, TGF-β, LAP, and CTLA-4 (data not shown). Low-dose peptide therapy did not change the overall phenotypes of $CD4^+CD25^+$ T or $CD8^+$ T cells, when compared with the same subsets isolated from control SNF1 mice (data not shown), indicating that a small percentage of autoantigen-specific T_{reg} cells are induced.

The autoepitope peptides that are effective in low-dose therapy contain class I epitopes

The nucleosomal histone peptides having MHC class II epitopes stimulate $CD4^+$ autoimmune Th cells of lupus (5–7, 9). Because $CD8^+$ T_{reg} cells were also induced by these autoepitopes, we looked for MHC class I-binding motifs, as described elsewhere (22, 23). Proteasomal cleavage probability and MHC-peptide-binding scores were assigned by computer prediction (http://www.mpiib-berlin.mpg.de/MAPPP/). We considered motifs with scores >0.5 as class I epitopes. The highest overall score for the sequence (bold, underlined) in the peptide containing the motif for binding to each class I molecule of the H-2^d haplotype is shown (the SNF1 mice are H-$2^{d/q}$ in haplotype): $H4_{71-94}$ TYTEHAKRK TV**<u>TAMDVVYAL</u>**KRQG (K^d, and L^d motif); K^d: cleavage probability: 1.0, binding score: 0.42, overall score: 0.71; L^d: cleavage probability:1.0, binding score: 0.32, overall score: 0.66; $H4_{16-39}$ KRHRKVLRD**<u>NIQGITKPA</u>**IRRLAR (K^d motif); K^d: cleavage probability:1.0, binding score: 0.34, overall score: 0.67; KR**<u>HRKVLRDNI</u>**QGITKPAIRRLAR (L^d motif); L^d: cleavage probability: 1.0, binding score: 0.30, overall score: 0.64; and $H1'_{22-42}$ STDHP**<u>KYSDMIVAA</u>**IQAEKNR (K^d motif); K^d: cleavage probability:1.0, binding score: 0.53, overall score: 0.76.

Low-dose therapy does not cause generalized immunosuppression

SNF1 mice were tolerized with $H4_{71-94}$ peptide or saline as control. Ten days after the third injection, the mice were immunized with HEL in CFA (100 μg/mouse) twice at 2-wk intervals. Seven days after the second immunization, the mice were bled to measure anti-HEL Ab response. Low-dose peptide-tolerized mice actually produced a 2-fold higher titer of anti-HEL Ab than control mice (Fig. 7). Moreover, IFN-γ or IL-2 response to in vitro rechallenge with HEL was actually increased in low-dose peptide-tolerized mice than in control mice ($p < 0.01$), but responses to anti-CD3 were similar in both groups ($p > 0.2$, Fig. 7 and data not shown).

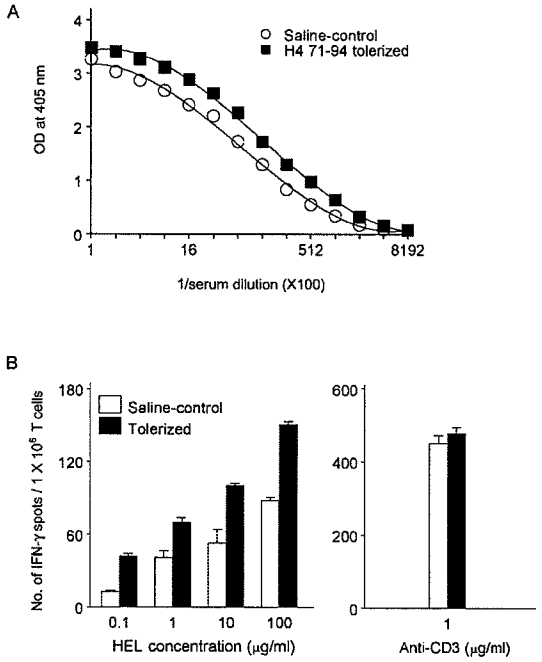

FIGURE 7. Low-dose tolerance therapy does not cause generalized immunosuppression. Control or low-dose peptide ($H4_{71-94}$)-tolerized SNF1 mice were immunized with HEL in CFA and then immune responses to HEL in both groups were compared (five mice per group). *A*,. Anti-HEL Ab responses were analyzed by ELISA. *B*,. IFN-γ responses to HEL or anti-CD3 Ab were measured by ELISPOT. Results are expressed as mean ± SEM from three experiments.

Discussion

Our studies indicate that nucleosomal-histone peptide epitopes are suitable for Ag-specific tolerance therapy of lupus. Nucleosome is one of the major immunogens driving lupus autoimmunity in murine and human SLE (2, 5, 7, 24, 25). Critical peptide epitopes from nucleosomal histones are recognized by autoimmune T cells of lupus patients, irrespective of their MHC haplotypes (5–7). The peptide epitopes are derived from a highly conserved, ubiquitous self-Ag, which is a product of ongoing apoptosis in generative lymphoid organs. Therefore, we have not observed any anaphylactic/allergic reactions with these peptides when used either for immunization or for tolerance therapy in >1000 SNF1 mice. Our peptides, administered s.c. in a very low-dose regimen, generate T_{reg} cells that suppress by TGF-β and/or by cell contact rather than causing Th2 deviation with allergic reactions seen in the case of peptide therapy of experimental autoimmune encephalomyelitis/multiple sclerosis and NOD diabetes (26, 27). Beneficial effects of our peptides outlast their short half-life by generating longer-lasting T_{reg} cells.

Thus, only 1 μg of nucleosomal histone peptide ($H1'_{22-42}$, $H4_{16-39}$, or $H4_{71-94}$) injected s.c. every 2 wk to SNF1 mice with clinically overt lupus could restore the life span to normal (~2 year) by markedly delaying death from severe nephritis. This s.c. dosage is 300- to 1000-fold lower than what we have previously used for i.v. nucleosomal peptide therapy (8) and what others have applied with anti-DNA autoantibody V region and related peptides (28–30). After 3 mo of low-dose $H1'_{22-42}$, $H4_{16-39}$, or $H4_{71-94}$ peptide treatment, IgG autoantibodies against nuclear Ags were reduced up to 90–100% as compared with controls after 3-mo therapy, indicating impairment of pathogenic T cell help. Interestingly, IgG deposits were observed in kidneys from both tolerized

and control mice, which did not correlate with their serum autoantibody levels. However, perivascular and interstitial infiltrations of mononuclear cells containing T, B, and plasma cells were markedly decreased in the peptide-tolerized SNF1 mice in contrast to control mice. Thus, very low-dose peptide therapy especially prevented local inflammatory damage in kidneys possibly by diminishing migration and activation of nephritogenic T and B cells, which might share antigenic specificities with the cells responsible for autoantibody production in the periphery.

Consistent with previous work, we found that pathogenic lupus T cells responding to nucleosomal epitopes are mainly IFN-γ-producing Th1 cells (5, 6). Each peptide treatment cross-reactively suppressed responses by lupus T cells to other peptide epitopes in addition to the tolerizing peptide and to nucleosomes, the major lupus immunogen containing many autoepitopes. A single peptide from a histone in the nucleosome can be recognized by multiple autoimmune T cells with diverse TCRs and, conversely, a single autoimmune T cell can promiscuously recognize multiple nucleosomal peptides that are structurally different (5, 8, 9). Thus, a single epitope may tolerize multiple autoimmune Th cells and tolerizing one set of Th cells would deprive help for a broad spectrum of autoimmune B cells (tolerance spreading). The suppression of the IFN-γ response to autoantigens was dose dependent, demonstrating autoantigen specificity, but it was overcome at higher doses, as in other systems (31). Increased production of TGF-β by T_{reg} cells upon stimulation with nucleosomal peptide and lack of suppression of the immune response to foreign Ag (HEL) immunization, again indicates that the peptide therapy generated autoantigen-specific T_{reg} cells. Moreover, suppression of help in autoantibody production by the T_{reg} cells also required the presence of nucleosomes (autoantigenic stimulation) in the helper-suppression assay cultures.

Thus, the low-dose nucleosomal peptide therapy repairs deficiencies of TGF-β-producing cells and $CD8^+$ T_{reg} function that has been observed in SLE (32–36). Unlike the case in organ-specific autoimmunity (15, 31, 37), the role of $CD4^+CD25^+$ T_{reg} in spontaneous SLE is controversial (38), but they could be potently induced by our therapy. We found that IL-10 is not involved in suppression of lupus with the low-dose peptide therapy. Like high-dose tolerance i.v. (8), nasal tolerance with one of the autoepitopes, $H4_{71-94}$, also could delay or treat lupus nephritis in SNF1 mice, but by generating IL-10-producing T cells (39). IL-10-producing T_{reg} cells might benefit lupus with some caveats (30, 40).

The $CD4^+CD25^+$ T_{reg} population could contain a subset of T cells that were secondarily induced to produce TGF-β, which suppresses autoimmunity (13, 32, 35, 41, 42). $CD8^+$ T_{reg} cells induced by low-dose tolerance were not CTL because they suppressed across membranes, even though the autoepitope peptides inducing such T_{reg} cells contained class I-binding motifs. Thus, the $CD8^+$ T_{reg} cells we have induced by nucleosomal peptides are different from the TCR clonotype-specific and cytotoxic suppressor cells in other systems (20, 22, 43–45). TGF-β produced by the $CD8^+$ T cells could have induced some of the $CD4^+CD25^+$ T_{reg} cells in our system. Indeed, the suppressive effect of these adaptive T_{reg} cells were similar at 1:1, 1:10, or 1:100 ratios (suppressor: target), suggesting involvement of "infectious tolerance" mechanisms, as in other systems (12, 42). We are in the process of studying how a combination of $CD4^+CD25^+$ and $CD8^+$ T_{reg} cells could interact in our low-dose peptide tolerance system, as exemplified in a graft-versus-host disease model (46). Although our long-term studies with spontaneous lupus disease were in progress (see footnote #2), another group induced a $CD4^+CD25^+$ subset of T_{reg} cells by continuous infusion of a model Ag in low doses (47).

Thus, although lupus T cells are resistant to classical anergy induction (48–50), tolerance therapy with select nucleosomal peptides still works by generating suppressive T_{reg} cells that impair T cell help for production of a broad spectrum of pathogenic autoantibodies and especially inhibit inflammatory insults in the lupus kidney. Moreover, these T_{reg} cells induced by very low-dose tolerance could possibly suppress activated dendritic cells and other APC in lupus (51, 52).

Acknowledgments

We thank Dr. Ethan Shevach (National Institutes of Health, Bethesda, MD) for critically reviewing our work and providing helpful suggestions.

Disclosures

The authors have no financial conflict of interest.

References

1. Wyllie, A. H. 1980. Glucocorticoid-induced thymocyte apoptosis is associated with endogenous endonuclease activation. *Nature 284:555.*
2. Mohan, C., S. Adams, V. Stanik, and S. K. Datta. 1993. Nucleosome: a major immunogen for the pathogenic autoantibody-inducing T cells of lupus. *J. Exp. Med. 177:1367.*
3. Datta, S. K., H. Patel, and D. Berry. 1987. Induction of a cationic shift in IgG anti-DNA autoantibodies: role of T helper cells with classical and novel phenotypes in three murine models of lupus nephritis. *J. Exp. Med. 165:1252.*
4. Shivakumar, S., G. C. Tsokos, and S. K. Datta. 1989. T cell receptor α/β expressing double negative ($CD4^-/CD8^-$) and $CD4^+$ T helper cells in humans augment the production of pathogenic anti-DNA autoantibodies associated with lupus nephritis. *J. Immunol. 143:103.*
5. Kaliyaperumal, A., C. Mohan, W. Wu, and S. K. Datta. 1996. Nucleosomal peptide epitopes for nephritis-inducing T helper cells of murine lupus. *J. Exp. Med. 183:2459.*
6. Kaliyaperumal, A., M. A. Michaels, and S. K. Datta. 2002. Naturally processed chromatin peptides reveal a major autoepitope that primes pathogenic T and B cells of lupus. *J. Immunol. 168:2530.*
7. Lu, L., A. Kaliyaperumal, D. T. Boumpas, and S. K. Datta. 1999. Major peptide autoepitopes for nucleosome-specific T cells of human lupus. *J. Clin. Invest. 104:345.*
8. Kaliyaperumal, A., M. A. Michaels, and S. K. Datta. 1999. Antigen-specific therapy of murine lupus nephritis using nucleosomal peptides: tolerance spreading impairs pathogenic function of autoimmune T and B cells. *J. Immunol. 162:5775.*
9. Shi, Y., A. Kaliyaperumal, L. Lu, S. Southwood, A. Sette, M. A. Michaels, and S. K. Datta. 1998. Promiscuous presentation and recognition of nucleosomal autoepitopes in lupus: role of autoimmune T cell receptor α chain. *J. Exp. Med. 187:367.*
10. Datta, S. K. 2003. Major peptide autoepitopes for nucleosome-centered T and B cell interaction in human and murine lupus. *Ann. NY Acad. Sci. 987:79.*
11. Nakamura, K., A. Kitani, and W. Strober. 2001. Cell contact-dependent immunosuppression by $CD4^+CD25^+$ regulatory T cells is mediated by cell surface-bound transforming growth factor β. *J. Exp. Med. 194:629.*
12. Zheng, S. G., Gray, J. D., Ohtsuka, K., Yamagiwa, S., Horwitz, D. A. 2002. Generation ex vivo of TGF-β-producing regulatory T cells from $CD4^+CD25^-$ precursors. *J. Immunol. 169:4183.*
13. Nakamura, K., A. Kitani, I. Fuss, A. Pedersen, N. Harada, H. Nawata, and W. Strober. 2004. TGF-β1 plays an important role in the mechanism of $CD4^+CD25^+$ regulatory T cell activity in both humans and mice. *J. Immunol. 172:834.*
14. Salomon, B., D. J. Lenschow, L. Rhee, N. Ashourian, B. Singh, A. Sharpe, and J. A. Bluestone. 2000. B7/CD28 costimulation is essential for the homeostasis of the $CD4^+CD25^+$ immunoregulatory T cells that control autoimmune diabetes. *Immunity 12:431.*
15. Hori, S., T. Nomura, and S. Sakaguchi. 2003. Control of regulatory T cell development by the transcription factor Foxp3. *Science 299:1057.*
16. Singh, R. R., V. Saxena, S. Zang, L. Li, F. D. Finkelman, D. P. Witte, and C. O. Jacob. 2003. Differential contribution of IL-4 and STAT6 vs STAT4 to the development of lupus nephritis. *J. Immunol. 170:4818.*
17. Schiffer, L., J. Sinha, X. Wang, W. Huang, G. von Gersdorff, M. Schiffer, M. P. Madaio, and A. Davidson. 2003. Short term administration of costimulatory blockade and cyclophosphamide induces remission of systemic lupus erythematosus nephritis in NZB/W F_1 mice by a mechanism downstream of renal immune complex deposition. *J. Immunol. 171:489.*
18. Gavalchin, J., and S. K. Datta. 1987. The NZB × SWR model of lupus nephritis. II. Autoantibodies deposited in renal lesions show a restricted idiotypic diversity. *J. Immunol. 138:138.*
19. Vlahakos, D., M. H. Foster, A. A. Ucci, K. J. Barrett, S. K. Datta, and M. P. Madaio. 1992. Murine monoclonal anti-DNA antibodies penetrate cells, bind to nuclei and induce glomerular proliferation and proteinuria in vivo. *J. Am. Soc. Nephrol. 2:1345.*
20. Najafian, N., T. Chitnis, A. D. Salama, B. Zhu, C. Benou, X. Yuan, M. R. Clarkson, M. H. Sayegh, and S. J. Khoury. 2003. Regulatory functions of $CD8^+CD28^-$ T cells in an autoimmune disease model. *J. Clin. Invest. 112:1037.*

21. Shimizu, J., S. Yamazaki, T. Takahashi, Y. Ishida, and S. Sakaguchi. 2002. Stimulation of $CD25^+CD4^+$ regulatory T cells through GITR breaks immunological self tolerance. *Nat. Immunol. 3:135.*
22. Fan, G.-C., and R. R. Singh. 2002. Vaccination with minigenes encoding V_H-derived major histocompatibility complex class I-binding epitopes activates cytotoxic T cells that ablate autoantibody-producing B cells and inhibit lupus. *J. Exp. Med. 196:731.*
23. Kuttler, C., A. K. Nussbaum, T. P. Dick, H. G. Rammensee, H. Schild, and K. P. Hadeler. 2000. An algorithm for the prediction of proteasomal cleavages. [Published erratum appears in *2000 J. Mol. Biol. 301:229.*]. *J. Mol. Biol. 298:417.*
24. Suen, J.-L., Y.-H. Chuang, B.-Y. Tsai, P. M. Yau, and B.-L. Chiang. 2004. Treatment of murine lupus using nucleosomal T cell epitopes identified by bone marrow-derived dendritic cells. *Arthritis Rheum. 50:3250.*
25. Fournel, S., S. Neichel, H. Dali, S. Farci, B. Maillere, J. P. Briand, and S. Muller. 2003. $CD4^+$ T cells from (New Zealand Black × New Zealand White)F_1 lupus mice and normal mice immunized against apoptotic nucleosomes recognize similar Th cell epitopes in the C terminus of histone H3. *J. Immunol. 171:636.*
26. Bielekova, B., B. Goodwin, N. Richert, I. Cortese, T. Kondo, G. Afshar, B. Gran, J. Eaton, J. Antel, J. A. Frank, H. F. McFarland, and R. Martin. 2000. Encephalitogenic potential of the myelin basic protein peptide (amino acids 83–99) in multiple sclerosis: results of a Phase II clinical trial with an altered peptide ligand. *Nat. Med. 6:1167.*
27. Liu, E., H. Moriyama, N. Abiru, D. Miao, L. Yu, R. M. Taylor, F. D. Finkelman, and G. S. Eisenbarth. 2002. Anti-peptide autoantibodies and fatal anaphylaxis in NOD mice in response to insulin self-peptides B:9–23 and B:13–23. *J. Clin. Invest. 110:1021.*
28. Hahn, B. H., R. R. Singh, W. K. Wong, B. P. Tsao, K. Bulpitt, and F. M. Ebling. 2001. Treatment with a consensus peptide based on amino acid sequences in autoantibodies prevents T cell activation by autoantigens and delays disease onset in murine lupus. *Arthritis Rheum. 44:432.*
29. Zinger, H., E. Eilat, A. Meshorer, and E. Mozes. 2003. Peptides based on the complementarity-determining regions of a pathogenic autoantibody mitigate lupus manifestations of (NZB × NZW)F_1 mice via active suppression. *Int. Immunol. 15:205.*
30. Riemekasten, G., D. Langnickel, P. Enghard, R. Undeutsch, J. Humrich, F. M. Ebling, B. Hocher, T. Humaljoki, H. Neumayer, G.-R. Burmester, et al. 2004. Intravenous injection of a D1 protein of the Smith proteins postpones murine lupus and induces type 1 regulatory T cells. *J. Immunol. 173:5835.*
31. Viglietta, V., C. Baecher-Allan, H. L. Weiner, and D. A. Hafler. 2004. Loss of functional suppression by $CD4^+CD25^+$ regulatory T cells in patients with multiple sclerosis. *J. Exp. Med. 199:971.*
32. Ohtsuka, K., J. D. Gray, M. M. Stimmler, B. Toro, and D. A. Horwitz. 1998. Decreased production of TGF-β by lymphocytes from patients with systemic lupus erythematosus. *J. Immunol. 160:2539.*
33. Filaci, G., S. Bacilieri, M. Fravega, M. Monetti, P. Contini, M. Ghio, M. Setti, F. Puppo, and F. Indiveri. 2001. Impairment of $CD8^+$ T suppressor cell function in patients with active systemic lupus erythematosus. *J. Immunol. 166:6452.*
34. Shustov, A., I. Luzina, P. Nguyen, J. C. Papadimitriou, B. Handwerger, K. B. Elkon, and C. S. Via. 2000. Role of perforin in controlling B-cell hyperactivity and humoral autoimmunity. *J. Clin. Invest. 106: R39.*
35. Singh, R. R., F. M. Ebling, D. A. Albuquerque, V. Saxena, V. Kumar, E. H. Giannini, T. N. Marion, F. D. Finkelman, and B. H. Hahn. 2002. Induction of autoantibody production is limited in nonautoimmune mice. *J. Immunol. 169:587.*
36. Stohl, W., J. E. Elliott, L. Li, E. R. Podack, D. H. Lynch, and C. O. Jacob. 1997. Impaired nonrestricted cytolytic activity in systemic lupus erythematosus: involvement of a pathway independent of Fas, tumor necrosis factor, and extracellular ATP that is associated with little detectable perforin. *Arthritis Rheum. 40:1130.*
37. Piccirillo, C. A., J. J. Letterio, A. M. Thornton, R. S. McHugh, M. Mamura, H. Mizuhara, and E. M. Shevach. 2002. $CD4^+CD25^+$ regulatory T cells can mediate suppressor function in the absence of transforming growth factor β1 production and responsiveness. *J. Exp. Med. 196:237.*
38. Bagavant, H., C. Thompson, K. Ohno, Y. Setiady, and K. S. K. Tung. 2002. Differential effect of neonatal thymectomy on systemic and organ-specific autoimmune disease. *Int. Immunol. 14:1397.*
39. Wu, H. Y., F. J. Ward, and N. A. Staines. 2002. Histone Peptide-induced nasal tolerance: suppression of murine lupus. *J. Immunol. 169:1126.*
40. Yin, Z., G. Bahtiyar, N. Zhang, L. Liu, P. Zhu, M. E. Robert, J. McNiff, M. P. Madaio, and J. Craft. 2002. IL-10 regulates murine lupus. *J. Immunol. 169:2148.*
41. Weiner, H. L. 2001. Induction and mechanism of action of transforming growth factor-β-secreting Th3 regulatory cells. *Immunol. Rev. 182:207.*
42. Chen, W., W. Jin, N. Hardegen, K. J. Lei, L. Li, N. Marinos, G. McGrady, and S. M. Wahl. 2003. Conversion of peripheral $CD4^+CD25^-$naive T cells to $CD4^+CD25^+$ regulatory T cells by TGF-β induction of transcription factor Foxp3. *J. Exp. Med. 198:1875.*
43. Jiang, H., N. S. Braunstein, B. Yu, R. Winchester, and L. Chess. 2001. $CD8^+$ T cells control the TH phenotype of MBP-reactive $CD4^+$ T cells in EAE mice. *Proc. Natl. Acad. Sci. USA 98:6301.*
44. Madakamutil, L. T., I. Maricic, E. Sercarz, and V. Kumar. 2003. Regulatory T cells control autoimmunity in vivo by inducing apoptotic depletion of activated pathogenic lymphocytes. *J. Immunol. 170:2985.*
45. Karandikar, N. J., M. P. Crawford, X. Yan, R. B. Ratts, J. M. Brenchley, D. R. Ambrozak, A. E. Lovett-Racke, E. M. Frohman, P. Stasny, D. C. Douek, et al. 2002. Glatiramer acetate (Copaxone) therapy induces $CD8^+$ T cell responses in patients with multiple sclerosis. *J. Clin. Invest. 109:641.*
46. Zheng, S. G., J. H. Wang, M. N. Koss, F. Quismorio, Jr., J. D. Gray, and D. A. Horwitz. 2004. $CD4^+$ and $CD8^+$ regulatory T cells generated ex vivo with IL-2 and TGF-β suppress a stimulatory graft-versus-host disease with a lupus-like syndrome. *J. Immunol. 172:1531.*
47. Apostolou, I., and H. von Boehmer. 2004. In vivo instruction of suppressor commitment in naive T cells. *J. Exp. Med. 199:1401.*
48. Yi, Y., M. McNerney, and S. K. Datta. 2000. Regulatory defects in Cbl and mitogen-activated protein kinase (extracellular signal-related kinase) pathways cause persistent hyperexpression of CD40 ligand in human lupus T cells. *J. Immunol. 165:6627.*
49. Bouzahzah, F., S. Jung, and J. Craft. 2003. $CD4^+$ T cells from lupus-prone mice avoid antigen-specific tolerance induction in vivo. *J. Immunol. 170:741.*
50. Xu, L., L. Zhang, Y. Yi, H. K. Kang, and S. K. Datta. 2004. Human lupus T cells resist inactivation and escape death by upregulating COX-2. *Nat. Med. 10:411.*
51. Blanco, P., A. K. Palucka, M. Gill, V. Pascual, and J. Banchereau. 2001. Induction of dendritic cell differentiation by IFN-α in systemic lupus erythematosus. *Science 294:1540.*
52. Kalled, S. L., A. H. Cutler, and L. C. Burkly. 2001. Apoptosis and altered dendritic cell homeostasis in lupus nephritis are limited by anti-CD154 treatment. *J. Immunol. 167:1740.*

Attachment 5

BAFF, a Novel Ligand of the Tumor Necrosis Factor Family, Stimulates B Cell Growth

By Pascal Schneider,* Fabienne MacKay,¶ Véronique Steiner,* Kay Hofmann,‡ Jean-Luc Bodmer,* Nils Holler,* Christine Ambrose,¶ Pornsri Lawton,¶ Sarah Bixler,¶ Hans Acha-Orbea,* Danila Valmori,§ Pedro Romero,§ Christiane Werner-Favre,‖ Rudolph H. Zubler,‖ Jeffrey L. Browning,¶ and Jürg Tschopp*

*From the *Institute of Biochemistry, University of Lausanne and ‡Swiss Institute for Experimental Cancer Research, BIL Research Centre, CH-1066 Epalinges, Switzerland; the §Division for Clinical Onco-Immunology, Ludwig Institute for Cancer Research, CHUV, CH-1011 Lausanne, Switzerland; the ‖Division of Haematology, Geneva University Hospital, CMU, 1211 Geneva 14, Switzerland; and ¶Biogen, Inc., Department of Immunology and Inflammation, Cambridge, Massachusetts 02142*

Summary

Members of the tumor necrosis factor (TNF) family induce pleiotropic biological responses, including cell growth, differentiation, and even death. Here we describe a novel member of the TNF family, designated BAFF (for B cell activating factor belonging to the TNF family), which is expressed by T cells and dendritic cells. Human BAFF was mapped to chromosome 13q32-34. Membrane-bound BAFF was processed and secreted through the action of a protease whose specificity matches that of the furin family of proprotein convertases. The expression of BAFF receptor appeared to be restricted to B cells. Both membrane-bound and soluble BAFF induced proliferation of anti-immunoglobulin M–stimulated peripheral blood B lymphocytes. Moreover, increased amounts of immunoglobulins were found in supernatants of germinal center–like B cells costimulated with BAFF. These results suggest that BAFF plays an important role as costimulator of B cell proliferation and function.

Key words: tumor necrosis factor • B lymphocytes • T lymphocytes • B cell growth • immunoglobulin G

Members of the TNF cytokine family are critically involved in the regulation of inflammation, of the immune response to infections, and of tissue homeostasis (1). The family members are type II membrane proteins that can act in a membrane-bound form or as proteolytically processed, soluble cytokines in an autocrine, paracrine, or endocrine manner (1). Binding of the ligands to their respective receptors induces oligomerization, initiating downstream signaling events.

Signaling pathways stimulated by TNF ligand members are diverse, including the activation of caspases, the translocation of nuclear factor (NF)-κB,[1] or the activation of mitogen-activated protein kinases such as c-Jun NH_2-terminal kinase (JNK) or extracellular signal regulatory kinase (ERK) (1). Thus, TNF-related ligands can lead to apoptosis, differentiation, or proliferation. Presently 16 members of the TNF-cytokine family have been described, several among them having important regulatory roles in function and development of the immune system. For instance, TNF acts as an inflammatory cytokine coordinating host defenses in response to infection (2). The lymphotoxin (LT) system is crucial in the development of peripheral lymphoid organs and the organization of splenic architecture (3, 4). Fas ligand (FasL, CD95L), TNF, and CD30L are responsible for TCR-mediated apoptosis of T cells and of immature thymocytes (5–7). Several of the TNF members and their receptors, in conjunction with TCR stimulation, also enhance T cell proliferation. Therefore, upregulation of TNF cytokine members and their receptors by TCR-induced signals can provide an autocrine costimulatory mechanism to increase the lymphocyte's own proliferation after stimulation with the antigen. However, upregulation of TNF-related ligands on T cells is also important for the activation

P. Schneider and F. MacKay contributed equally to this work.

[1] *Abbreviations used in this paper:* aa, amino acid(s); APRIL, a proliferation inducing ligand; BAFF, B cell activating factor belonging to the TNF family; EST, expressed sequence tag; LT, lymphotoxin; NF, nuclear factor; PNGase F, peptide *N*-glycanase F; RANKL, receptor activator of NF-κB ligand; TRAIL, TNF-related apoptosis-inducing ligand; wt, wild-type.

 J. Exp. Med. © The Rockefeller University Press • 0022-1007/99/06/1747/10 $2.00
Volume 189, Number 11, June 7, 1999 1747–1756
http://www.jem.org

and stimulation of neighboring cells. For example, CD40L is important for B cell survival, proliferation, Ig isotype switch, and differentiation (8), and the interaction of OX40 with OX40L is necessary for the differentiation of activated B cells into high Ig-producing cells (9).

Here we characterize the structural and functional properties of a new ligand of the TNF cytokine family. The new ligand, termed BAFF (B cell activating factor belonging to the TNF family), appears to be expressed by T cells and dendritic cells for the purpose of B cell costimulation, and may therefore play an important role in the control of B cell function.

Materials and Methods

Materials. The anti-Flag M2 mAb, biotinylated anti-Flag M2 antibody, and the anti-Flag M2 antibody coupled to agarose were purchased from Sigma Chemical Co. Cell culture reagents were obtained from Life Sciences and BioWhittaker. Flag-tagged soluble human APRIL (a proliferation inducing ligand; residues K_{110}–L_{250}) was produced in 293 cells as described (10, 11). FITC-labeled anti-CD4, anti-CD8, and anti-CD19 antibodies were purchased from PharMingen. Goat $F(ab')_2$ specific for the $Fc_{5\mu}$ fragment of human IgM were purchased from Jackson ImmunoResearch Laboratories. Secondary antibodies were obtained from either PharMingen or Jackson ImmunoResearch Laboratories and were used at the recommended dilutions.

Cells. Human embryonic kidney 293 T cells (12) and fibroblast cell lines (see Table I) were maintained in DMEM containing 10% heat-inactivated FCS. Human embryonic kidney 293 cells were maintained in DMEM-nutrient mix F12 (1:1) supplemented with 2% FCS. T cell lines, B cell lines, and macrophage cell lines (see Table I) were grown in RPMI supplemented with 10% FCS. Molt-4 cells were cultivated in Iscove's medium supplemented with 10% FCS. Epithelial cell lines were grown in MEM-α medium containing 10% FCS, 0.5 mM nonessential amino acids, 10 mM Na-Hepes, and 1 mM Na pyruvate. Human umbilical vein endothelial cells were maintained in M199 medium supplemented with 20% FCS, 100 μg/ml of epithelial cell growth factor (Collaborative Research, Inotech), and 100 μg/ml of heparin sodium salt (Sigma Chemical Co.). All media contained penicillin and streptomycin antibiotics.

PBLs were isolated from heparinized blood of healthy adult volunteers by Ficoll-Paque (Amersham Pharmacia Biotech) gradient centrifugation and cultured in RPMI, 10% FCS.

T cells were obtained from nonadherent PBLs by rosetting with neuraminidase-treated sheep red blood cells and separated from nonrosetting cells (mostly B cells) by Ficoll-Paque gradient centrifugation. Purified T cells were activated for 24 h with phytohemagglutinin (1 μg/ml; Sigma Chemical Co.), washed, and cultured in RPMI, 10% FCS, 20 U/ml of IL-2. $CD14^+$ monocytes were purified by magnetic cell sorting using anti-CD14 antibodies, goat anti-mouse-coated microbeads, and a Minimacs™ device (Miltenyi Biotech), and cultivated in the presence of GM-CSF (800 U/ml, Leucomax®; Essex Chemie) and IL-4 (20 ng/ml; Lucerna Chem) for 5 d, then with GM-CSF, IL-4, and TNF-α (200 U/ml; Bender) for an additional 3 d to obtain a $CD83^+$, dendritic cell–like population.

Human B cells of >97% purity were isolated from peripheral blood or umbilical cord blood using anti-CD19 magnetic beads (M450; Dynal) as described (13).

Northern Blot. Northern blot analysis was carried out using Human Multiple Tissue Northern Blots I and II (7760-1 and 7759-1; Clontech). The membranes were incubated in hybridization solution (50% formamide, 2.5× Denhardt's, 0.2% SDS, 10 mM EDTA, 2× SSC, 50 mM NaH_2PO_4, pH 6.5, 200 μg/ml sonicated salmon sperm DNA) for 2 h at 60°C. Antisense RNA probe containing the nucleotides corresponding to amino acids (aa) 136–285 of human BAFF (hBAFF) was heat denatured and added at 2×10^6 cpm/ml in fresh hybridization solution. The membrane was hybridized 16 h at 62°C, washed once in 2× SSC, 0.05% SDS (30 min at 25°C), once in 0.1× SSC, 0.1% SDS (20 min at 65°C), and exposed at −70°C to x-ray films.

Characterization of BAFF cDNA. A partial sequence of hBAFF cDNA was contained in several expressed sequence tag (EST) clones (sequence data available from EMBL/GenBank/DDBJ under accession nos. T87299 and AA166695) derived from fetal liver and spleen and ovarian cancer libraries. The 5′ portion of the cDNA was obtained by 5′ rapid amplification of cDNA ends (RACE) PCR (Marathon-Ready cDNA; Clontech) with oligonucleotides AP1 and JT1013 (5′-ACTGTTTCTTCTGGACCC-TGAACGGC-3′) using the provided cDNA library from a pool of human leukocytes as template, as recommended by the manufacturer. The resulting PCR product was cloned into PCR-0 blunt (Invitrogen) and subcloned as EcoRI-PstI fragment into pT7T3 Pac vector (Amersham Pharmacia Biotech) containing EST clone T87299. Therefore, full-length hBAFF cDNA was obtained by combining 5′ and 3′ fragments using the internal PstI site of BAFF. The sequence has been assigned EMBL/GenBank/DDBJ accession no. AF116456.

A partial 617-bp sequence of murine BAFF was contained in two overlapping EST clones (EMBL/GenBank/DDBJ accession nos. AA422749 and AA254047). A PCR fragment spanning nucleotides 158–391 of this sequence was used as a probe to screen a mouse spleen cDNA library (Stratagene, Inc.). The sequence has been assigned EMBL/GenBank/DDBJ accession no. AF119383.

Expression of Recombinant BAFF. Full-length hBAFF was amplified using oligos JT1069 (5′-GACAAGCTTGCCACCATG-GATGACTCCACA-3′) and JT637 (5′-ACTAGTCACAGCA-GTTTCAATGC-3′). The PCR product was cloned into PCR-0 blunt and resubcloned as HindIII-EcoRI fragment into PCR-3 mammalian expression vector. A short version of soluble BAFF (sBAFF/short, aa Q136–L285) was amplified using oligos JT636 (5′-CTGCAGGGTCCAGAAGAAACAG-3′) and JT637. A long version of sBAFF (sBAFF/long, aa L83–L285) was obtained from full-length BAFF using internal PstI site. sBAFFs were resubcloned as PstI-EcoRI fragments behind the hemagglutinin signal peptide and Flag sequence of a modified PCR-3 vector, and as PstI-SpeI fragments into a modified pQE16 bacterial expression vector in frame with an NH_2-terminal Flag sequence (14). Constructs were sequenced on both strands.

The establishment of stable 293 cell lines expressing the short soluble form or full-length BAFF, and the expression and purification of recombinant sBAFF from bacteria and mammalian 293 cells were performed as described (14, 15).

Reverse Transcriptase PCR. Total RNA extracted from T cells, B cells, in vitro–derived immature dendritic cells, 293 wild-type (wt) and 293-BAFF (full-length) cells was reverse transcribed using the Ready to Go system (Amersham Pharmacia Biotech) according to the manufacturer's instructions. BAFF and β-actin cDNAs were detected by PCR amplification with Taq DNA polymerase (steps of 1 min each at 94°C, 55°C, and 72°C for 30 cycles) using specific oligonucleotides: for BAFF, JT1322 5′-GGAGAAG-GCAACTCCAGTCAGAAC-3′ and JT1323 5′-CAATTCATC-

CCCAAAGACATGGAC-3′; for IL-2 receptor α chain, JT1368 5′-TCGGAACACAACGAAACAAGTC-3′ and JT1369 5′-CTTCTCCTTCACCTGGAAACTGACTG-3′; and for β-actin, 5′-GGCATCGTGATGGACTCCG-3′ and 5′-GCTGGAAGGTGGACAGCGA-3′.

Gel Permeation Chromatography. 293 T cells were transiently transfected with the short form of sBAFF and grown in serum-free Optimem medium for 7 d. Conditioned supernatants were concentrated 20 times, mixed with internal standards catalase and OVA, and loaded onto a Superdex-200 HR10/30 column. Proteins were eluted in PBS at 0.5 ml/min, and fractions (0.25 ml) were precipitated with TCA and analyzed by Western blotting using anti-Flag M2 antibody. The column was calibrated with standard proteins: ferritin (440 kD), catalase (232 kD), aldolase (158 kD), BSA (67 kD), OVA (43 kD), chymotrypsinogen A (25 kD), and ribonuclease A (13.7 kD).

PNGase F Treatment. Samples were heated in 20 μl of 0.5% SDS, 1% 2-ME for 3 min at 95°C, then cooled and supplemented with 10% NP-40 (2 μl), 0.5 M sodium phosphate, pH 7.5 (2 μl), and Peptide *N*-glycanase F (PNGase F; 125 U/μl, 1 μl, or no enzyme in controls). Samples were incubated for 3 h at 37°C before analysis by Western blotting.

Edman Sequencing. 293 T cells were transiently transfected with the long form of sBAFF and grown in serum-free Optimem medium for 7 d. Conditioned supernatants were concentrated 20 times, fractionated by SDS-PAGE, and blotted onto polyvinylidene difluoride membrane (Bio-Rad Laboratories) as described previously (16), and then sequenced using a gas phase sequencer (ABI 120A; Perkin Elmer) coupled to an analyzer (ABI 120A; Perkin Elmer) equipped with a phenylthiohydantoin C18 2.1 × 250 mm column. Data were analyzed using ABI 610 software (Perkin Elmer).

Antibodies. Polyclonal antibodies were generated by immunizing rabbits (Eurogentec) with recombinant sBAFF/long. Spleens of rats immunized with the same antigen were fused to x63Ag8.653 mouse myeloma cells, and hybridomas were screened for BAFF-specific IgGs. One of these mAbs, 43.9, is an IgG2a that specifically recognizes hBAFF.

FACS®. Cells were stained in 50 μl of FACS buffer (PBS, 10% FCS, 0.02% NaN_3) with 50 ng (or the indicated amount) of Flag-tagged short soluble hBAFF for 20 min at 4°C, followed by anti-Flag M2 (1 μg) and secondary antibody. Anti-BAFF mAb 43.9 was used at 40 μg/ml. For two-color FACS® analysis, peripheral blood lymphocytes were stained with Flag-tagged sBAFF/long (2 μg/ml), followed by biotinylated anti-Flag M2 (1:400) and PE-labeled streptavidin (1:100), followed by FITC-labeled anti-CD4, anti-CD8, or anti-CD19.

PBL Proliferation Assay. PBLs were incubated in 96-well plates (10^5 cells/well in 100 μl RPMI supplemented with 10% FCS) for 72 h in the presence or absence of 2 μg/ml of goat anti–human μ chain antibody (Sigma Chemical Co.) or control $F(ab')_2$ and with the indicated concentration of native or boiled sBAFF/long. Cells were pulsed for an additional 6 h with [^{3}H]thymidine (1 μCi/well) and harvested. [^{3}H]Thymidine incorporation was monitored by liquid scintillation counting. In some experiments, recombinant sBAFF was replaced by 293 cells stably transfected with full-length BAFF (or 293 wild-type [wt] as control) that had been fixed for 5 min at 25°C in 1% paraformaldehyde. Assay was performed as described (17). In further experiments, $CD19^+$ cells were isolated from PBLs with magnetic beads, and the remaining $CD19^-$ cells were irradiated (3,000 rads) before reconstitution with $CD19^+$ cells. Proliferation assay with sBAFF was then performed as described above.

B Cell Activation Assay. Purified B cells were activated in the EL-4 culture system as described (13). In brief, 10^4 B cells mixed with 5 × 10^4 irradiated murine EL-4 thymoma cells (clone B5) were cultured for 5–6 d in 200 μl medium containing 5% vol/vol of culture supernatants from human T cells (10^6/ml) which had been activated for 48 h with PHA (1 μg/ml) and PMA (1 ng/ml). B cells were then reisolated with anti-CD19 beads and cultured for another 7 d (5 × 10^4 cells in 200 μl, duplicate or triplicate

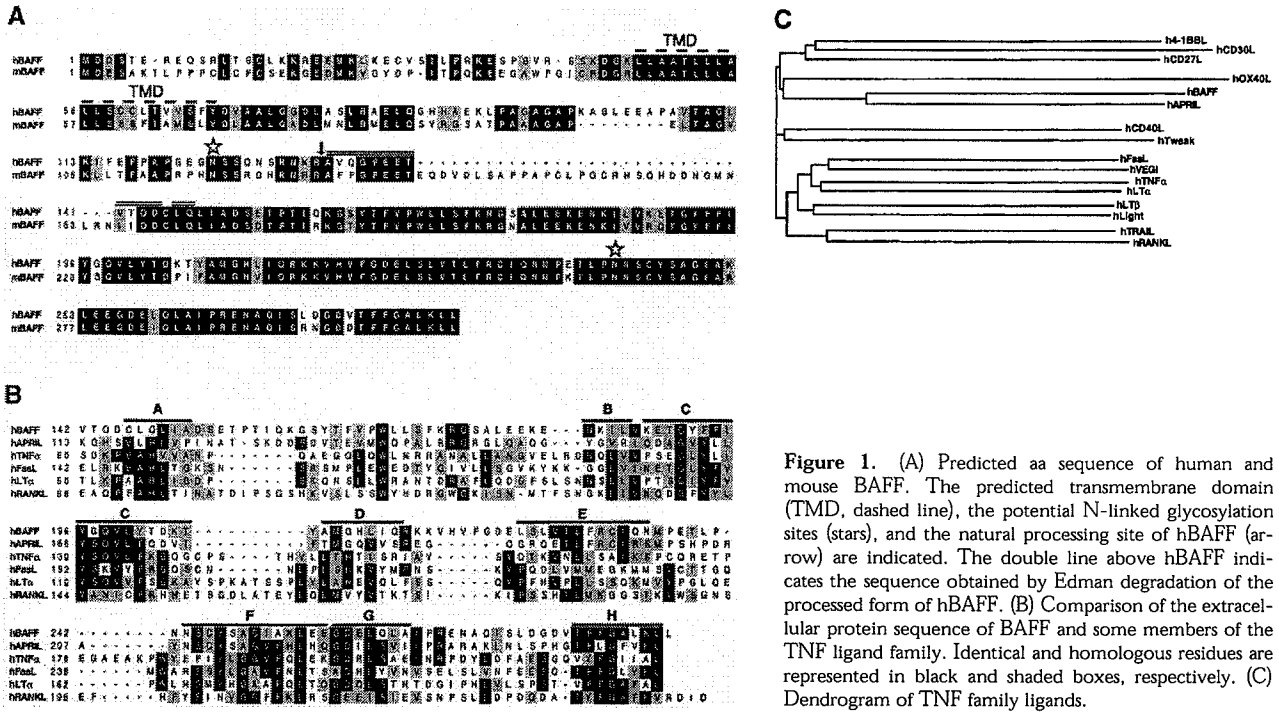

Figure 1. (A) Predicted aa sequence of human and mouse BAFF. The predicted transmembrane domain (TMD, dashed line), the potential N-linked glycosylation sites (stars), and the natural processing site of hBAFF (arrow) are indicated. The double line above hBAFF indicates the sequence obtained by Edman degradation of the processed form of hBAFF. (B) Comparison of the extracellular protein sequence of BAFF and some members of the TNF ligand family. Identical and homologous residues are represented in black and shaded boxes, respectively. (C) Dendrogram of TNF family ligands.

culture in flat-bottomed 96 well plates) in medium alone or in medium supplemented with 5% T cell supernatants, or with 50 ng/ml IL-2 (a gift from the former Glaxo Institute for Molecular Biology, Geneva) and 10 ng/ml each IL-4 and IL-10 (Pepro-Tech), in the presence or absence of sBAFF. The anti-Flag M2 antibody was added at a concentration of 2 μg/ml and had no effect by itself.

Results

BAFF Is a Novel Ligand of the TNF Family. hBAFF was identified by sequence homology as a possible novel member of the TNF ligand family while we screened public databases using an improved profile search (18). A cDNA encoding the complete protein of 285 aa was obtained by combining EST clones (covering the 3′ region) with a fragment (5′ region) amplified by PCR. The absence of a signal peptide suggested that BAFF was a type II membrane protein that is typical of the members of the TNF ligand family. The protein has a predicted cytoplasmic domain of 46 aa, a hydrophobic transmembrane region, and an extracellular domain of 218 aa containing two potential *N*-glycosylation sites (Fig. 1 A). The sequence of the extracellular domain of BAFF shows highest homology with APRIL (33% aa identity, 48% homology), whereas the identity with other members of the family, such as TNF, FasL, LTα, TRAIL (TNF-related apoptosis-inducing ligand), or RANKL (receptor activator of NF-κB ligand) is <20% (Fig. 1, B and C). The mouse BAFF (mBAFF) cDNA clone isolated from a spleen library encoded a slightly longer protein (309 aa) due to an insertion between the transmembrane region and the first of several β strands which constitute the receptor binding domain in all TNF ligand members (19). This β strand–rich ectodomain is almost identical in mBAFF and hBAFF (86% identity, 93% homology), suggesting that the BAFF gene has been highly conserved during evolution (Fig. 1 A).

BAFF Is Processed and Secreted. Although TNF family members are synthesized as membrane-inserted ligands, cleavage in the stalk region between transmembrane and receptor binding domains is frequently observed. For example, TNF and FasL are readily cleaved from the cell surface by metalloproteinases (20, 21). While producing several forms of recombinant BAFF in 293 T cells, we noticed that a recombinant soluble 32-kD form of BAFF (aa 83–285, sBAFF/long), containing the complete stalk region and an NH_2-terminal Flag tag in addition to the receptor binding domain, was extensively processed to a smaller 18-kD fragment (Fig. 2, A and B). Cleavage occurred in the stalk region since the fragment was detectable only with antibodies raised against the complete receptor interaction domain of BAFF but not with anti-Flag antibodies (data not shown). This experiment also revealed that only N124 (located in the stalk) but not N242 (located at the entry of the F-β sheet) was glycosylated, since the molecular mass of the nonprocessed sBAFF/long was reduced from 32 to 30 kD upon removal of the N-linked carbohydrates with PNGase F, whereas the 18-kD cleaved form was insensitive to this treatment. Peptide sequence analysis of the 18-kD fragment indeed showed that cleavage occurred between R133 and A134 (Fig. 1 A). R133 lies at the end of a polybasic region that is conserved between human (R-N-K-R) and mouse (R-N-R-R) BAFF. To test whether cleavage was not merely an artifact of expressing soluble, nonnatural forms of BAFF, membrane-bound full-length BAFF was expressed in 293 T cells (Fig. 2 C). The 32-kD complete BAFF and some higher molecular mass species (probably

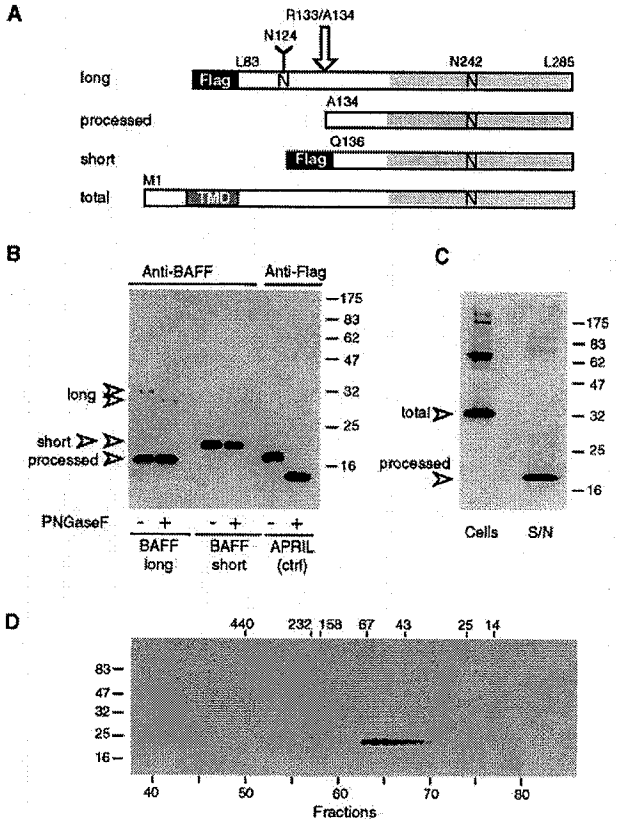

Figure 2. Characterization of recombinant BAFF. (A) Schematic representation of recombinant BAFF constructs. Soluble recombinant BAFFs starting at Leu_{83} and Gln_{136} are expressed fused to an NH_2-terminal Flag tag and a 6-amino acid linker. The long form is cleaved between Arg_{133} and Ala_{134} (arrow) in 293 T cells, to yield a processed form of BAFF. Asn_{124} and Asn_{242} belong to *N*-glycosylation consensus sites. N-linked glycan present on Asn_{124} is shown as a Y. TMD, transmembrane domain. (B) PNGase F treatment of recombinant BAFF. Concentrated supernatants containing Flag-tagged BAFFs and APRIL were deglycosylated and analyzed by Western blotting using polyclonal anti-BAFF antibodies or anti-Flag M2, as indicated. All bands except processed BAFF also reacted with anti-Flag M2 (data not shown). (C) Full-length BAFF is processed to a soluble form. 293 T cells were transiently transfected with full-length BAFF. Transfected cells and their concentrated supernatants (S/N) were analyzed by Western blotting using polyclonal anti-BAFF antibodies. Supernatants corresponding to 10 times the amount of cells were loaded onto the gel. (D) Size exclusion chromatography of sBAFF on Superdex-200. Concentrated supernatants containing sBAFF/short were fractionated on a Superdex-200 column, and the eluted fractions were analyzed by Western blotting using anti-Flag M2 antibody. The migration positions of the molecular mass markers (in kD) are indicated on the left-hand side for SDS-PAGE and at the top of the figure for size exclusion chromatography.

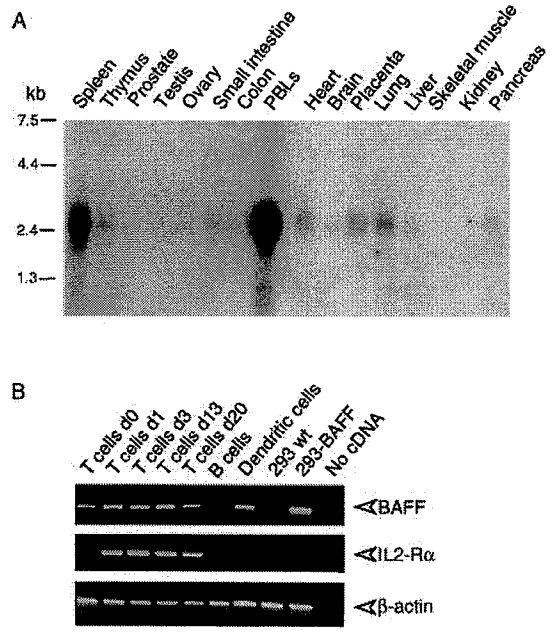

Figure 3. Expression of BAFF. (A) Northern blots (2 μg poly A^+ RNA per lane) of various human tissues were probed with BAFF antisense mRNA. (B) Reverse transcriptase amplification of BAFF, IL-2 receptor α chain (IL2-Rα), and actin from RNA of purified blood T cells at various time points of PHA activation, E-rosetting–negative blood cells (mostly B cells), in vitro–derived immature dendritic cells, 293 cells, and 293 cells stably transfected with full-length BAFF (293-BAFF). Control amplifications were performed in the absence of added cDNA. IL-2 receptor α chain was amplified as a marker of T cell activation.

corresponding to nondissociated dimers and trimers) were readily detectable in cellular extracts, but >95% of BAFF recovered from the supernatant corresponded to the processed 18-kD form, indicating that BAFF was also processed when synthesized as a membrane-bound ligand.

Therefore, we engineered an sBAFF (Q136–L285, sBAFF/short) whose sequence started 2 aa downstream of the processing site (Fig. 1 B). As predicted, the Flag tag attached to the NH_2 terminus of this recombinant molecule was not removed (data not shown), which allowed its purification by an anti-Flag affinity column. To test its correct folding, the purified sBAFF/short was analyzed by gel filtration where the protein eluted at an apparent molecular mass of 55 kD (Fig. 2 D). We conclude that sBAFF/short correctly assembles into a homotrimer (3 × 20 kD) in agreement with the quaternary structure of other TNF family members (19). Finally, unprocessed sBAFF/long was readily expressed in bacteria, indicating that the cleavage event was specific to eukaryotic cells.

Expression and Chromosomal Localization of BAFF. Northern blot analysis of BAFF revealed that the 2.5-kb BAFF mRNA was abundant in the spleen and PBLs (Fig. 3 A). Thymus, heart, placenta, small intestine, and lung showed weak expression. This restricted distribution suggested that cells present in lymphoid tissues were the main source of BAFF. Through PCR analysis, we found that BAFF mRNA was present in T cells and peripheral blood monocyte–derived dendritic cells but not in B cells (Fig. 3 B). Even naive, nonstimulated T cells appeared to express some BAFF mRNA.

A sequence-tagged site (STS, SHGC-36171) was found in the database which included the hBAFF sequence. This site maps to human chromosome 13, in a 9-cM interval between the markers D13S286 and D13S1315. On the cytogenetic map, this interval corresponds to 13q32-34. Of the known TNF ligand family members, only RANKL (Trance) has been localized to this chromosome (22) though quite distant to BAFF (13q14).

BAFF Receptor Is Expressed on B Cells. For the ligand to exert maximal biological effects, it was likely that the BAFF receptor (BAFF-R) would be expressed either on the same cells or on neighboring cells present in lymphoid tissues. Using the recombinant sBAFF as a tool to specifically determine BAFF-R expression by FACS®, we indeed found high levels of receptor expression in various B cell lines, such as the Burkitt lymphomas Raji and BJAB (Fig. 4 A, and Table I). In contrast, cell lines of T cell, fibroblastic, epithelial, and endothelial origin were all negative. Very weak staining was observed with the monocyte line THP-1, which, however, could be due to Fc receptor binding. Thus, BAFF-R expression appears to be restricted to B cell lines. The two mouse B cell lines tested were negative using the hBAFF as a probe, although weak binding was observed on mouse splenocytes (data not shown). The presence of BAFF-R on B cells was corroborated by analy-

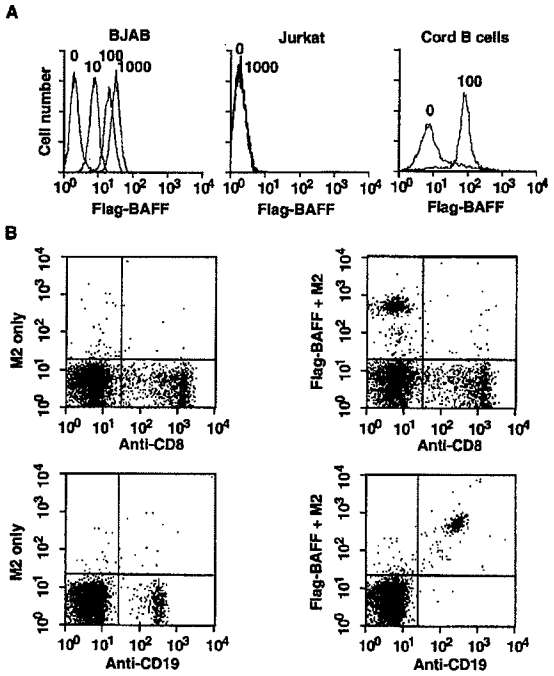

Figure 4. BAFF binds to mature B cells. (A) Binding of sBAFF to BJAB and Jurkat cell lines, and to purified $CD19^+$ cells of cord blood. Cells were stained with the indicated amount (in ng/50 μl) of Flag-BAFF and analyzed by flow cytometry. (B) Binding of sBAFF to PBLs. PBLs were stained with anti-CD8–FITC or with anti-CD19–FITC (x axis) and with Flag-BAFF plus M2-biotin and avidin-PE (y axis). Flag-BAFF was omitted in controls.

Table I. *Binding of sBAFF to Various Cell Lines*

Cell type	Cell lines	BAFF binding	Specific details
Epithelial-like	HT-29	−	Colon adenocarcinoma
	A375	−/+	Melanoma
	MCF-7	−	Breast adenocarcinoma
	Me260	−	Melanoma
	Cos	+	Monkey kidney cells
Fibroblasts	WI-38	−	Lung
	Hs-68	−	Foreskin
	Hs-27	−	Foreskin
Endothelial cells	HUVEC	−	Umbilical vein
Macrophages/monocytes	THP-1	−/+	Monocyte
T cell lines	Molt-4	−	Lymphoblastic leukemia
	Hut-78	−	Cutaneous lymphoma
	Jurkat	−	Lymphoblastic leukemia
B cell lines	BJAB	+++	Burkitt lymphoma
	Namalawa	++	Burkitt lymphoma
	Daudi	+/−	Burkitt lymphoma EBNA$^+$ VCA$^+$
	Ramos	++	Burkitt lymphoma EBV$^-$
	Raji	+++	Burkitt lymphoma
	JIYOYE	+	Burkitt lymphoma
	SKW.64	++	IgM secreting EBV$^+$
	RPMI 1788	+++	Peripheral blood, IgM secreting
	IM-9	+++	Lymphoblast Ig secreting
	NC-37	+++	Lymphoblast EBV$^+$
Mouse cell lines	WEHI-231	−	B cell lymphoma
	A20	−	B cell lymphoma

sis of umbilical cord and peripheral blood lymphocytes. While CD8$^+$ and CD4$^+$ T cells lacked BAFF-R (Fig. 4 B, and data not shown), abundant staining was observed on CD19$^+$ B cells (Fig. 4, A and B), indicating that BAFF-R is expressed on all blood B cells, including naive and memory B cells. No evidence was obtained for a CD19$^+$, BAFF-R$^-$ population.

BAFF Can Costimulate B Cell Growth. Since BAFF bound to blood-derived B cells, experiments were performed to determine whether the ligand could deliver growth-stimulatory or growth-inhibitory signals. PBLs were stimulated with anti-IgM (μ) antibodies together with fixed 293 cells stably expressing surface BAFF (Fig. 5 A). The levels of [^{3}H]thymidine incorporation induced by anti-μ alone were not altered by the presence of control cells but were increased twofold in the presence of BAFF-transfected cells (Fig. 5 B). A dose-dependent proliferation of PBLs was also obtained when BAFF-transfected cells were replaced by purified sBAFF (Fig. 5 C), indicating that BAFF does not require membrane attachment to exert its activity. In this experimental setup, proliferation induced by sCD40L required concentrations >1 μg/ml, but was less dependent on the presence of anti-μ than that mediated by BAFF (Fig. 5 D). When purified CD19$^+$ B cells were cocultured with irradiated autologous CD19$^-$ PBLs, costimulation of proliferation by BAFF was unaffected, demonstrating that [^{3}H]thymidine uptake was mainly due to B cell proliferation and not to an indirect stimulation of another cell type (data not shown). The observed B cell proliferation in response to BAFF was entirely dependent on the presence of anti-μ antibodies, indicating that BAFF functioned as costimulator of B cell proliferation.

To investigate a possible effect of BAFF on preplasma, germinal center–like B cells (13), purified peripheral or cord blood B cells were preactivated by coculture with EL-4 T cells in the presence of a cytokine mixture from supernatants of PHA/PMA-stimulated T cells (23). These B cells were reisolated to 98% purity and yielded a twofold increase in secreted Ig during a secondary culture in the presence of BAFF and activated T cell cytokines compared with cytokines alone. No significant effect was seen in the absence of exogenous cytokines, and an intermediate (1.5-fold) effect was observed in the presence of the recombinant cytokines IL-2, IL-4, and IL-10 (Fig. 5, E and F).

Discussion

Here we report the molecular cloning, expression, and biological activity of a new member of the TNF ligand

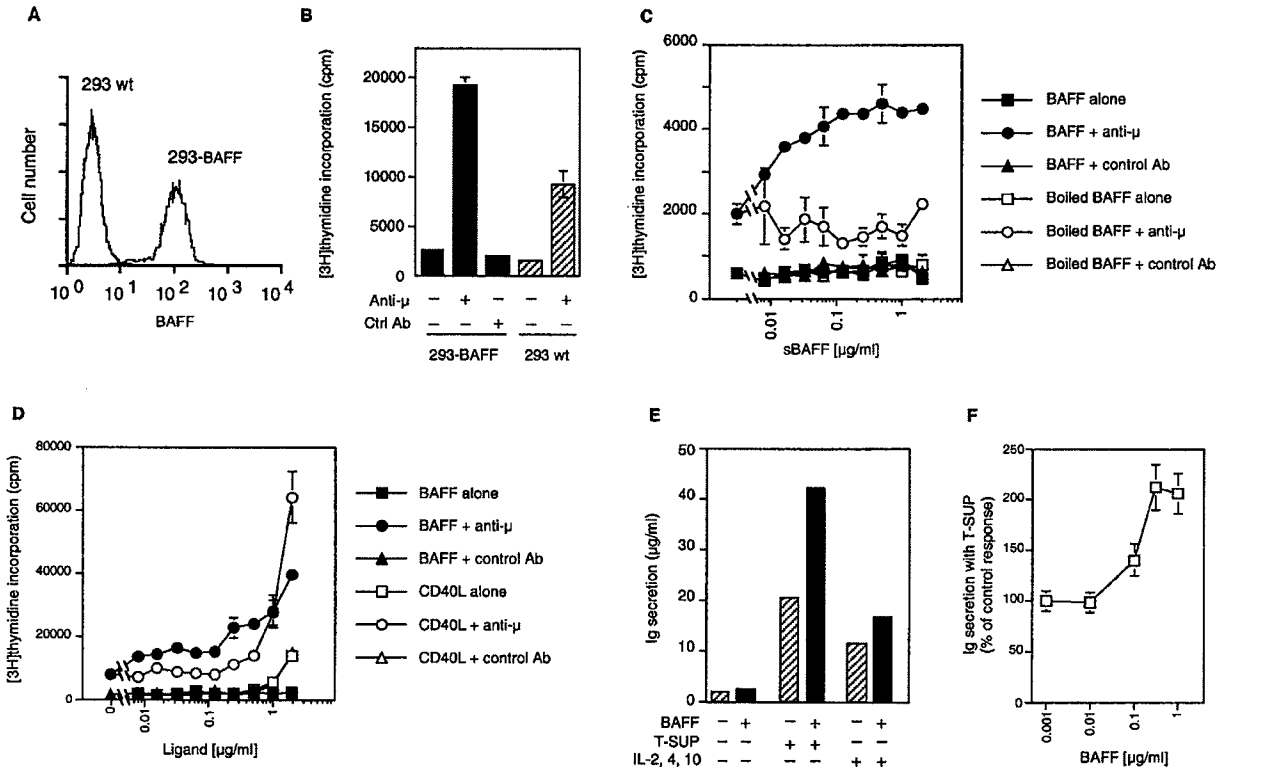

Figure 5. BAFF costimulates B cell proliferation. (A) Surface expression of BAFF in stably transfected 293 cells. 293-BAFF and 293 wt cells were stained with anti-BAFF mAb 43.9 and analyzed by flow cytometry. (B) Costimulation of PBLs by 293-BAFF cells. PBLs (10^5/well) were incubated with 15,000 paraformaldehyde-fixed 293 cells (293 wt or 293-BAFF) in the presence or absence of anti-B cell receptor antibody (anti-μ). Fixed 293 cells alone incorporated 100 cpm. (C) Dose-dependent costimulation of PBL proliferation by sBAFF in the presence of anti-μ. Proliferation was determined after 72 h incubation by [^{3}H]thymidine incorporation. Controls include cells treated with BAFF alone, with heat-denatured BAFF, or with an irrelevant isotype-matched antibody in place of anti-μ. (D) Comparison of (co)stimulatory effects of sCD40L and sBAFF on PBL proliferation. Experiment was performed as described in panel C. (E) BAFF costimulates Ig secretion of preactivated human B cells. Purified CD19$^+$ B cells were activated by coculture with EL-4 T cells and activated T cell supernatants for 5–6 d, then reisolated and cultured for another 7 d in the presence of medium only (−) or containing 5% activated T cell supernatants (T-SUP) or a blend of cytokines (IL-2, IL-4, IL-10). The columns represent means of Ig concentrations for cultures with or without 1 μg/ml BAFF. Means of fold increase ± SD were 1.23 ± 0.11 for medium only, 2.06 ± 0.18 with T cell supernatants (four experiments), and 1.45 ± 0.06 with IL-2, IL-4, and IL-10 (two experiments). These were performed with peripheral blood (three experiments) or cord blood B cells (one experiment; 2.3-fold increase with T cell supernatants, 1.5-fold increase with IL-2, IL-4, and IL-10). (F) Dose–response curve for the effect of BAFF in cultures with T cell supernatants, as shown in panel D. Mean ± SD of three experiments.

family. The human and mouse sequences exhibit the typical characteristics of this family, i.e., a type II membrane protein organization and the conservation of nine β sheets, which fold into a "jelly-roll" structure that trimerizes to form receptor interacting sites. The biochemical analysis of BAFF is also consistent with the typical homotrimeric structure of TNF family members. In this family of ligands, BAFF exhibits the highest level of sequence similarity with APRIL, which we have recently characterized as a ligand stimulating growth of various tumor cells (11). Unlike TNF and LTα, which are two family members with equally high homology (33% identity) and whose genes are linked on chromosome 6, APRIL and BAFF are not clustered on the same chromosome. APRIL is located on chromosome 17 (our unpublished data), whereas BAFF maps to the distal arm of human chromosome 13 (13q34). Abnormalities in this locus were characterized in Burkitt lymphomas as the second most frequent defect (24) besides the translocation involving the myc gene into the Ig locus (25). Considering the high expression levels of BAFF-R on all Burkitt lymphoma cell lines analyzed (see Table I), this raises the intriguing possibility that some Burkitt lymphomas may have deregulated BAFF expression, thus stimulating growth in an autocrine manner.

B cell growth was efficiently costimulated with recombinant sBAFF lacking the transmembrane domain. This activity is in contrast to several TNF family members that are active only as membrane-bound ligands, such as TRAIL, FasL, and CD40L. Soluble forms of these ligands have poor biological activity that can be enhanced by their cross-linking, thereby mimicking the membrane-bound ligand (15). In contrast, cross-linking Flag-tagged sBAFF with anti-Flag antibodies or the use of membrane-bound BAFF expressed on the surface of epithelial cells did not further enhance the mitogenic activity of BAFF, suggesting that it can act systemically as a secreted cytokine, like TNF does. This is in agreement with the observation that a polybasic sequence present in the stalk of BAFF acted as a substrate for a pro-

tease. Similar polybasic sequences are also present at corresponding locations in both APRIL and TWEAK (Apo-3L), and for both of them there is evidence of proteolytic processing (26; Holler, N., and J. Tschopp, unpublished observation). Although the protease responsible for the cleavage remains to be determined, it is unlikely to be the metalloproteinase responsible for the release of membrane-bound TNF, as their sequence preferences differ completely (21). The multibasic motifs in BAFF (R-N-K-R), APRIL (R-K-R-R), and TWEAK (R-P-R-R) are reminiscent of the minimal cleavage signal for furin (R-X-K/R-R), the prototype of a proprotein convertase family (27).

The role of antigen-specific B lymphocytes during the different stages of the immune response is highly dependent on signals and contacts from helper T cells (28) and antigen-presenting cells such as dendritic cells (29). B lymphocytes first receive these signals early on during the immune response when they interact with T cells at the edge of the B cell follicles in lymphoid tissues, leading to their proliferation and differentiation into low-affinity antibody-forming cells (30). At the same time, some antigen-specific B cells also migrate to the B cell follicle and contribute to the formation of germinal centers, another site of B cell proliferation but also affinity maturation and generation of memory B cells and high-affinity plasma cells (31).

Signals triggered by CD40L have been shown to be critical for the function of B lymphocytes at multiple steps of the T cell–dependent immune response (32). However, several studies clearly showed that CD40L–CD40 interaction does not account for all contact-dependent T cell help for B cells. Indeed, CD40L-deficient T cells isolated from either knockout mice or patients with X-linked hyper IgM syndrome have been shown to successfully induce proliferation of B cells and their differentiation into plasma cells (33). Likewise, studies using blocking antibodies against CD40L showed that a subset of surface IgD^+ B cells isolated from human tonsils proliferate and differentiate in response to activated T cells in a CD40-independent manner (34). Other members of the TNF family, such as membrane-bound TNF and CD30L, have also been shown to be involved in a CD40- and surface Ig–independent stimulation of B cells (33, 35). Finally, CD40-deficient B cells can be stimulated to proliferate and differentiate into plasma cells by helper T cells as long as the surface B cell receptors are triggered at the same time (36). BAFF as well as CD30L and CD40L is expressed by T cells, but its uniqueness resides in its expression by dendritic cells as well as the highly specific location of its receptor on B cells in contrast to the wider expression patterns of CD40, CD30, and the TNF receptors (37). Hence, BAFF may uniquely affect B cells.

In support of a role for BAFF in T cell– and/or dendritic cell–induced B cell growth and potential maturation, we found that BAFF costimulates proliferation of blood-derived B cells concomitantly with cross-linking of the B cell receptors. Moreover, using $CD19^+$ B cells differentiated in vitro into preplasma, germinal center–like B cells (13), we observed a costimulatory effect of BAFF on Ig production by these B cells in the presence of cytokines from activated T cells. Thus, BAFF can induce signals in both naive B cells and germinal center–committed B cells in vitro. Whether this observation will translate during a normal immune response or not will have to be addressed by proper in vivo experiments.

The biological responses induced in B cells by BAFF are distinct from that of CD40L, since proliferation triggered by CD40L occurred at a lower level independently of an anti-μ costimulus (17; Fig. 5 D). Moreover, CD40L can counteract apoptotic signals in B cells after engagement of the B cell receptor (38), whereas BAFF was not able to rescue the B cell line Ramos from anti-μ–mediated apoptosis, despite the fact that Ramos cells do express BAFF-R (Table I; MacKay, F., unpublished observations). Therefore, it is likely that CD40L and BAFF fulfill distinct functions. In this respect, it is noteworthy that BAFF did not interact with any of 16 recombinant receptors of the TNF family tested, including CD40 (Schneider, P., and J. Tschopp, unpublished observations).

Several obscure zones remain in our understanding of an immune response. For instance, little is known about the mechanisms governing the differentiation of a B cell into a plasma cell versus a germinal center B cell. Similarly, aside from the possible involvement of the CD40 pathway shown in vitro (39), we have very little information about the signals deciding the differentiation of a germinal center B cell into a memory B cell or a plasma cell. It will be very interesting to investigate whether or not BAFF has any unique role to play in these critical checkpoint decisions.

We thank S. Hertig (University of Lausanne), L. Scarpellino (University of Lausanne), and S. Foley (Biogen, Inc.) for technical assistance, Richard Tizard (Biogen, Inc.) and Brittney Colemen (Biogen, Inc.) for DNA sequencing, and Ralph Budd (University of Lausanne) for reading the manuscript.

This work was supported by grants from the Swiss National Science Foundation (to J. Tschopp) and the Swiss Federal Office of Public Health (to P. Schneider and J. Tschopp).

Address correspondence to Jürg Tschopp, Institute of Biochemistry, University of Lausanne, Ch. des Boveresses 155, CH-1066 Epalinges, Switzerland. Phone: 41-21-692-5738; Fax: 41-21-692-5705; E-mail: jurg.tschopp@ib.unil.ch

Received for publication 27 January 1999 and in revised form 17 March 1999.

References

1. Smith, C.A., T. Farrah, and R.G. Goodwin. 1994. The TNF-receptor superfamily of cellular and viral proteins: activation, costimulation, and death. *Cell.* 76:959–962.
2. Vassalli, P. 1992. The pathophysiology of tumor necrosis factors. *Annu. Rev. Immunol.* 10:411–452.
3. De Togni, P., J. Goellner, N.H. Ruddle, P.R. Streeter, A. Fick, S. Mariathasan, S.C. Smith, R. Carlson, L.P. Shornick, J. Strauss-Schoenberger, et al. 1994. Abnormal development of peripheral lymphoid organs in mice deficient in lymphotoxin. *Science.* 264:703–707.
4. Koni, P.A., R. Sacca, P. Lawton, J.L. Browning, N.H. Ruddle, and R.A. Flavell. 1997. Distinct roles in lymphoid organogenesis for lymphotoxins alpha and beta revealed in lymphotoxin beta-deficient mice. *Immunity.* 6:491–500.
5. Amakawa, R., A. Hakem, T.M. Kundig, T. Matsuyama, J.J. Simard, E. Timms, A. Wakeham, H.W. Mittruecker, H. Griesser, H. Takimoto, et al. 1996. Impaired negative selection of T cells in Hodgkin's disease antigen CD30-deficient mice. *Cell.* 84:551–562.
6. Russell, J.H., B. Rush, C. Weaver, and R. Wang. 1993. Mature T cells of the autoimmune lpr/lpr mice have a defect in antigen-stimulated suicide. *Proc. Natl. Acad. Sci. USA.* 90: 4409–4413.
7. Zheng, L., G. Fisher, R.E. Miller, J. Peschon, D.H. Lynch, and M.J. Lenardo. 1995. Induction of apoptosis in mature T cells by tumor necrosis factor. *Nature.* 377:348–351.
8. van Kooten, C., and J. Banchereau. 1997. Functions of CD40 on B cells, dendritic cells and other cells. *Curr. Opin. Immunol.* 9:330–337.
9. Stuber, E., and W. Strober. 1996. The T cell–B cell interaction via OX40–OX40L is necessary for the T cell–dependent humoral immune response. *J. Exp. Med.* 183:979–989.
10. Schneider, P., J.L. Bodmer, N. Holler, C. Mattmann, P. Scuderi, A. Terskikh, M.C. Peitsch, and J. Tschopp. 1997. Characterization of Fas (Apo-1, CD95)-Fas ligand interaction. *J. Biol. Chem.* 272:18827–18833.
11. Hahne, M., T. Kataoka, M. Schroter, K. Hofmann, M. Irmler, J.L. Bodmer, P. Schneider, T. Bornand, N. Holler, L.E. French, et al. 1998. APRIL, a new ligand of the tumor necrosis factor family, stimulates tumor cell growth. *J. Exp. Med.* 188:1185–1190.
12. Hahne, M., D. Rimoldi, M. Schroter, P. Romero, M. Schreier, L.E. French, P. Schneider, T. Bornand, A. Fontana, D. Lienard, et al. 1996. Melanoma cell expression of Fas(Apo-1/CD95) ligand: implications for tumor immune escape. *Science.* 274:1363–1366.
13. Grimaitre, M., C. Werner-Favre, V. Kindler, and R.H. Zubler. 1997. Human naive B cells cultured with EL-4 T cells mimic a germinal center-related B cell stage before generating plasma cells. Concordant changes in Bcl-2 protein and messenger RNA levels. *Eur. J. Immunol.* 27:199–205.
14. Thome, M., P. Schneider, K. Hofmann, H. Fickenscher, E. Meinl, F. Neipel, C. Mattmann, K. Burns, J.L. Bodmer, M. Schroter, et al. 1997. Viral FLICE-inhibitory proteins (FLIPs) prevent apoptosis induced by death receptors. *Nature.* 386:517–521.
15. Schneider, P., N. Holler, J.L. Bodmer, M. Hahne, K. Frei, A. Fontana, and J. Tschopp. 1998. Conversion of membrane-bound Fas(CD95) ligand to its soluble form is associated with downregulation of its proapoptotic activity and loss of liver toxicity. *J. Exp. Med.* 187:1205–1213.
16. Matsudaira, P. 1987. Sequence from picomole quantities of proteins electroblotted onto polyvinylidene difluoride membranes. *J. Biol. Chem.* 262:10035–10038.
17. Armitage, R.J., W.C. Fanslow, L. Strockbine, T.A. Sato, K.N. Clifford, B.M. Macduff, D.M. Anderson, S.D. Gimpel, T. Davis-Smith, C.R. Maliszewski, et al. 1992. Molecular and biological characterization of a murine ligand for CD40. *Nature.* 357:80–82.
18. Bucher, P., K. Karplus, N. Moeri, and K. Hofmann. 1996. A flexible search technique based on generalized profiles. *Comp. Chem.* 20:3–23.
19. Banner, D.W., A. D'Arcy, W. Janes, R. Gentz, H.J. Schoenfeld, C. Broger, H. Loetscher, and W. Lesslauer. 1993. Crystal structure of the soluble human 55 kd TNF receptor-human TNF beta complex: implications for TNF receptor activation. *Cell.* 73:431–445.
20. Nagata, S. 1997. Apoptosis by death factor. *Cell.* 88:355–365.
21. Black, R.A., C.T. Rauch, C.J. Kozlosky, J.J. Peschon, J.L. Slack, M.F. Wolfson, B.J. Castner, K.L. Stocking, P. Reddy, S. Srinivasan, et al. 1997. A metalloproteinase disintegrin that releases tumour-necrosis factor-alpha from cells. *Nature.* 385: 729–733.
22. Wong, R., J. Rho, J. Arron, E. Robinson, J. Orlinick, M. Chao, S. Kalachikov, E. Cayani, F. Bartlett, W. Frankel, et al. 1997. TRANCE is a novel ligand of the tumor necrosis factor receptor family that activates c-Jun N-terminal kinase in T cells. *J. Biol. Chem.* 272:25190–25194.
23. Kindler, V., and R.H. Zubler. 1997. Memory, but not naive, peripheral blood B lymphocytes differentiate into Ig-secreting cells after CD40 ligation and costimulation with IL-4 and the differentiation factors IL-2, IL-10, and IL-3. *J. Immunol.* 159:2085–2090.
24. Berger, R., M. Le Coniat, J. Derre, and D. Vecchione. 1989. Secondary nonrandom chromosomal abnormalities of band 13q34 in Burkitt lymphoma-leukemia. *Genes Chromosomes Cancer.* 1:115–118.
25. Magrath, I. 1990. The pathogenesis of Burkitt's lymphoma. *Adv. Cancer Res.* 55:133–270.
26. Chicheportiche, Y., P.R. Bourdon, H. Xu, Y.M. Hsu, H. Scott, C. Hession, I. Garcia, and J.L. Browning. 1997. TWEAK, a new secreted ligand in the tumor necrosis factor family that weakly induces apoptosis. *J. Biol. Chem.* 272: 32401–32410.
27. Nakayama, K. 1997. Furin: a mammalian subtilisin/Kex2p-like endoprotease involved in processing of a wide variety of precursor proteins. *Biochem. J.* 327:625–635.
28. Hodgkin, P.D., and A. Basten. 1995. B cell activation, tolerance and antigen-presenting function. *Curr. Opin. Immunol.* 7:121–129.
29. Dubois, B., B. Vanbervliet, J. Fayette, C. Massacrier, C. Van Kooten, F. Briere, J. Banchereau, and C. Caux. 1997. Dendritic cells enhance growth and differentiation of CD40-activated B lymphocytes. *J. Exp. Med.* 185:941–951.
30. Garside, P., E. Ingulli, R.R. Merica, J.G. Johnson, R.J. Noelle, and M.K. Jenkins. 1998. Visualization of specific B and T lymphocyte interactions in the lymph node. *Science.* 281: 96–99.
31. MacLennan, I.C., A. Gulbranson-Judge, K.M. Toellner, M. Casamayor-Palleja, E. Chan, D.M. Sze, S.A. Luther, and H.A. Orbea. 1997. The changing preference of T and B cells for partners as T-dependent antibody responses develop. *Immunol. Rev.* 156:53–66.
32. Grewal, I.S., and R.A. Flavell. 1998. CD40 and CD154 in

cell-mediated immunity. *Annu. Rev. Immunol.* 16:111–135.
33. Armitage, R.J., and M.R. Alderson. 1995. B-cell stimulation. *Curr. Opin. Immunol.* 7:243–247.
34. Blanchard, D., C. Gaillard, P. Hermann, and J. Banchereau. 1994. Role of CD40 antigen and interleukin-2 in T cell-dependent human B lymphocyte growth. *Eur. J. Immunol.* 24:330–335.
35. Shanebeck, K.D., C.R. Maliszewski, M.K. Kennedy, K.S. Picha, C.A. Smith, R.G. Goodwin, and K.H. Grabstein. 1995. Regulation of murine B cell growth and differentiation by CD30 ligand. *Eur. J. Immunol.* 25:2147–2153.
36. Schrader, C.E., J. Stavnezer, H. Kikutani, and D.C. Parker. 1997. Cognate T cell help for CD40-deficient B cells induces c-myc RNA expression, but DNA synthesis requires an additional signal through surface Ig. *J. Immunol.* 158:153–162.
37. Gruss, H.J., and S.K. Dower. 1995. Tumor necrosis factor ligand superfamily: involvement in the pathology of malignant lymphomas. *Blood.* 85:3378–3404.
38. Tsubata, T., J. Wu, and T. Honjo. 1993. B-cell apoptosis induced by antigen receptor crosslinking is blocked by a T-cell signal through CD40. *Nature.* 364:645–648.
39. Arpin, C., J. Dechanet, C. Van Kooten, P. Merville, G. Grouard, F. Briere, J. Banchereau, and Y.J. Liu. 1995. Generation of memory B cells and plasma cells in vitro. *Science.* 268:720–722.